This is an open access article published under a Creative Commons Attribution (CC-BY) License, which permits unrestricted use, distribution and reproduction in any medium, provided the author and source are cited.

ACS AUTHORCHOICE

ACS Catalysis

pubs.acs.org/acscatalysis

Review

Propylene Epoxidation using Molecular Oxygen over Copper- and Silver-Based Catalysts: A Review

Janvit Teržan, Matej Huš, Blaž Likozar, and Petar Djinović*

Cite This: *ACS Catal.* 2020, 10, 13415–13436

Read Online

ACCESS | Metrics & More | Article Recommendations

ABSTRACT: Propylene oxide (PO) is a versatile chemical, mainly used in the synthesis of polyurethane plastics. Propylene epoxidation using molecular oxygen could replace the tedious current synthesis protocols, which use expensive H_2O_2 or organic peroxides as oxidants. This review focuses on the propylene epoxidation reaction using molecular oxygen in the gas phase over copper- and silver-based catalysts. Silver is a proven and industrially used ethylene epoxidation catalyst. However, it initiates allylic hydrogen stripping (AHS) in propylene epoxidation, shifting the selectivity toward unwanted acrolein and total oxidation. Nevertheless, silver has been extensively studied to determine if AHS could be mitigated by targeted active site design and various doping strategies. Copper-based catalysts have been less extensively studied but have been experimentally proved as well as theoretically confirmed that their PO selectivity is on par with that of silver. In this review, different catalyst modification strategies have been analyzed and the achieved improvements discussed. Theoretical approaches aimed at understanding the mechanism and predicting catalytic performance on the basis of electronic states (density functional theory calculations) are also reviewed. We conclude with a future outlook on how the current state of the art knowledge of active site modification and reaction engineering approaches could leverage the PO selectivity toward industrial requirements, thus enabling a breakthrough in gas-phase propylene epoxidation using O_2.

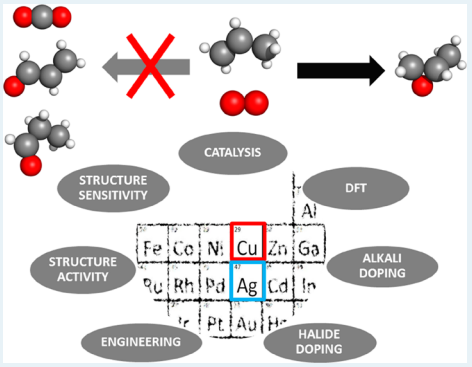

KEYWORDS: *catalytic epoxidation, propylene, molecular oxygen, selectivity, silver, copper oxide, reaction mechanism*

Downloaded via 92.37.61.195 on November 26, 2020 at 09:58:09 (UTC).
See https://pubs.acs.org/sharingguidelines for options on how to legitimately share published articles.

1. INTRODUCTION

Propene (C_3H_6), commonly referred to as propylene (as it will be referred to in this work), is produced during oil refining as a result of cracking of larger hydrocarbons. In the last two decades, extensive exploitation of shale gas, which contains a notable fraction of C3 and C4 alkanes, has revived the industrial and academic interest in propane dehydrogenation (to propylene) and consequently selective propylene oxidation reactions.

In the presence of oxygen and a suitable catalyst, propylene can be oxidized to several oxygenates (Figure 1). Total oxidation is thermodynamically favored but undesired, as cheaper fuels with a higher energy density exist for power/heat generation. The technology for partial oxidation of propylene to C3 oxygenates (acrolein, propanal, 1-propanol, isopropanol, and acetone) is known and is performed on an industrial scale with sufficient selectivity.[1−4]

Propylene oxide (PO) is a colorless volatile liquid with a high commercial value ($10.5 billion market value in 2017).[5] It is a raw material in the manufacturing of polyurethane foams (furniture and automobile seating, insulation foams, and food packaging). This accounts for about 60% of the propylene oxide used.[6] The rest is hydrolyzed to propylene glycol (about 20%[6]), which is used as a solvent or has niche uses, such as a fixating agent in microscopy, fumigant, etc.[6] Population growth, accompanied by increasing living standards, is the driving force behind the rising demand for propylene oxide. Projections show that by 2025 the annual PO demand will exceed 20 Mt.[7]

There are several established techniques for PO synthesis; however, all of them have environmental or economic issues (Figure 2).

The chlorohydrin process (CHPO) is most widely used. To avoid using chlorine in the chlorohydrin process, epoxidation of propylene using organic hydroperoxides has been implemented. The organic intermediates used are ethylbenzene (PO/SM), isobutene (PO/TBA) (Figure 2), or cumene (CHP).[7] First, the intermediate molecule is peroxidized, and the product is then used to epoxidize propylene to PO. The drawback when isobutene or ethylbenzene is used (Figure 2) is that while the coproducts

Received: July 31, 2020
Revised: October 10, 2020
Published: November 4, 2020

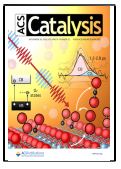

© 2020 American Chemical Society

https://dx.doi.org/10.1021/acscatal.0c03340
ACS Catal. 2020, 10, 13415−13436

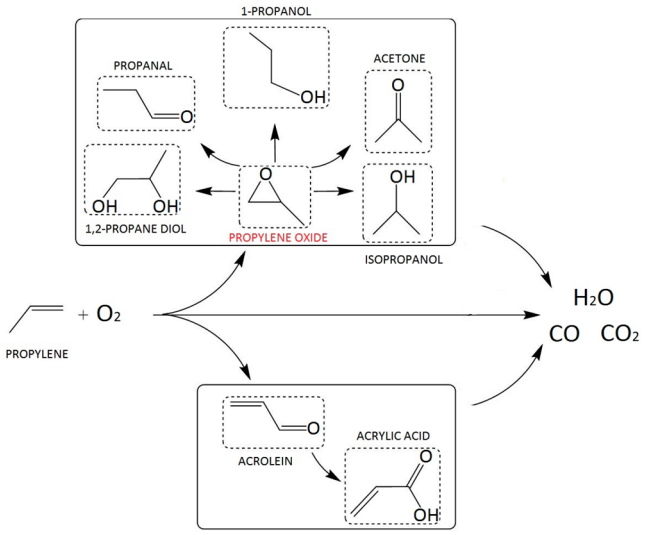

Figure 1. Reaction pathways of total and partial oxidation of propylene into various C3 oxygenates.

(styrene and *tert*-butanol) have some economic value, they are produced in large quantities that exceed the market demand. The cumene process (CHP) has the advantage that dimethylphenylmethanol, the coproduct in the process, can be recycled to cumene by dehydration and hydrogenation. In 2008, Evonik (formerly Degussa) commercialized a process (HPPO) where H_2O_2 is used to directly epoxidize propylene (with over 90% PO selectivity) over a TS-1 catalyst, with water being the only side product. However, the 2019 cost of H_2O_2 (~500 USD/t) is relatively high in comparison to that of PO (~1500 USD/t), which is a major economic downside of this process.[8,9] As a result, oxidation by abundant and cheap oxygen is highly preferred, but a suitable catalytic process that can selectively epoxidize propylene is still unknown.

The idea of propylene epoxidation by molecular oxygen is not new by any means. A thorough work by Khatib et al.[8] reviewed numerous catalysts, reactor types, means of energy input (thermal and light), and oxidants used (O_2, N_2O) for propylene epoxidation. More recently, Blanckenberg and Malgas-Enus[10] reviewed the epoxidation of several alkenes over transition-metal nanocatalysts. The reactions reported were mainly performed in the liquid phase, often with H_2O_2 as the oxidant.

During the selective propylene epoxidation reaction, oxygen atom insertion into the C=C double bond of propylene is an electrophilic addition reaction. On the other hand, the main (and dominant) competitive reaction is allylic hydrogen stripping (AHS), which is a dehydrogenation reaction involving nucleophilic oxygen species and produces acrolein. This means that the electrophilic/nucleophilic character of the oxidizing species is crucial to govern the reaction selectivity. The selectivity toward PO is still the main bottleneck of the reaction, which coupled with relatively low catalytic activity gives PO yields well below 5%.[8] In addition, there are several additional properties of a catalyst that need to be considered to improve PO selectivity: the presence of acidic sites, the geometry of the active site,[11] electronic or dipole perturbation of the Ag or CuO_x surface induced by alkali or halide ion modification, etc. These parameters are important, as the electron-donating or -withdrawing affinity (acidity/basicity) of the surface, as well as surface atom arrangement, strongly influence the mode of oxygen activation, giving rise to surface oxygen species with different reactivities and selectivities. Also, excessive catalyst (support) acidity can cause PO isomerization, which leads to loss of selectivity.

This review covers original scientific papers as well as patent literature and will focus on experimental, DFT, and engineering approaches aimed at improving PO selectivity over silver- and copper-based catalysts.

2. EXPERIMENTAL PROPYLENE EPOXIDATION ON SILVER-BASED CATALYSTS

Conventionally synthesized bulk or supported metal nanoparticle catalysts are typically polycrystalline: they exhibit

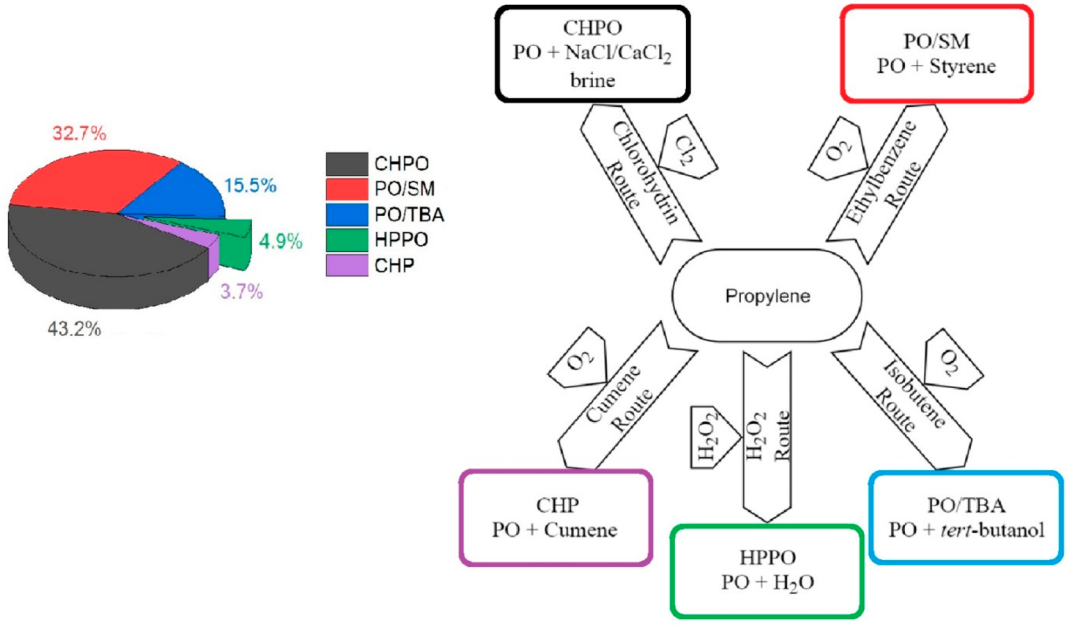

Figure 2. Industrial propylene oxide production processes and fraction of PO produced through them.

https://dx.doi.org/10.1021/acscatal.0c03340
ACS Catal. 2020, 10, 13415−13436

several crystallographic facets, have different abundances of edge and kink sites, and often show a broad particle size distribution. This makes an experimental analysis of the active and (non)selective sites a daunting task. To circumvent the effect of polydispersity, valuable information can be obtained from surface studies of single crystals.

Pulido et al.[12] analyzed oxygen activation and propylene epoxidation by a temperature-programmed reaction coupled by Raman and mass spectroscopy (MS) over Ag(111) and Ag(100) single crystals. On the Ag(111) surface, oxygen activation started at 225 °C and Raman bands appeared at 475, 875, 957, and 990 cm^{-1}, which were assigned to monatomic oxygen (Ag−O), hydroxyl (Ag−OH), and molecular oxygen (O═O), respectively. When the temperature was raised to 250 °C, two new weak bands appeared at 603 and 790 cm^{-1}, associated with subsurface oxo species and surface oxygen. Oxygen activation on the Ag(100) facet started at a lower temperature: at 200 °C, bands at 338, 470, 604, 802, 870, and 957 cm^{-1} were observed. At 250 °C, the Raman spectra on both Ag(100) and Ag(111) surfaces showed quite similar oxygen species.

On the Ag(100) facet, acrolein, CO_2, acetone, and propylene oxide (and/or propanal) were observed in the investigated reaction temperature range (200−275 °C). However, with the Ag(111) catalyst, the dominant product was CO_2 (acetone, propanal, and PO were ruled out) in the whole range of temperatures studied, indicating that only the allylic route was accessible. The experimental single crystal studies were complemented by DFT studies to further an understanding using data that was inaccessible by analytical techniques. Among the several O_2 adsorption complexes investigated on the Ag(100) surface with oxygen coverage 0.222, the most stable complex had each of the two oxygen atoms bridged between two silver atoms and 65 kJ mol^{-1} was released in the adsorption process. O_2 dissociation was exothermic by 119 kJ mol^{-1} and required an activation energy of about 90 kJ mol^{-1}. The relative energy of the most stable O_2 adsorption complex on the Ag(111) surface with respect to gas-phase O_2 and the silver surface was only 21 kJ mol^{-1}. The activation energy required to dissociate O_2 on the Ag(111) surface was about 20 kJ mol^{-1} larger than that on the Ag(100) surface, and the reaction was exothermic by 101 kJ mol^{-1}. Modeling the propylene oxidation mechanism over the Ag(111) and Ag(100) surfaces suggested the product distribution observed experimentally.

Ranney et al.[13] investigated the Ag(110) facet, which is the most active low-index silver surface for oxygen adsorption. The presence of adsorbed oxygen increased the energy required for desorbing both propylene and propylene oxide, resulting in a deep oxidation of the adsorbed propylene. When water was coadsorbed on the oxygen-populated Ag(110) surface (resulting in hydroxyl group formation), the combustion of adsorbed propylene was avoided and the activation energy for desorption of both propylene and PO was reduced.

Single-crystal studies have shed light onto structure−activity differences of different Ag facets, which are attainable for practical applications by a controlled synthesis of nanoshaped silver particles, such as cubes, spheres, etc.[14] In this way, the abundance of active sites can be greatly increased in comparison to single-crystal studies (based on the increase of specific surface area of nanopowders vs single crystals). Despite a clear supremacy of Ag cubes over spheres and wires for ethylene epoxidation selectivity,[15] experimental evidence for propylene epoxidation is still missing. Yu et al.[14] synthesized Ag cubes and spheres (both ∼45 nm in size), but no experimental comparison of bulk nanopowders in propylene oxidation was shown. When they were supported over La_2O_3, the Ag cubes greatly outperformed the Ag nanospheres, which is in accordance with the single-crystal studies of Pulido et al.[12]

Using temperature-programmed desorption (TPD), MS, and IR spectroscopy, Henriques et al.[16] tested two bulk silver catalysts, prepared by calcination of a silver nitrate/ammonia solution precipitate and reduction of bulk Ag_2O. They showed that the selectivity toward epoxides (ethylene/propylene) can be increased by decreasing the amount of surface-bound oxygen. The higher epoxide yield stems not from the increased epoxidation selectivity but instead from the decreased CO_2 formation. This means that a further total oxidation of PO has a crucial effect that lowers the PO yield. The decomposition of the epoxides upon readsorption on the catalyst proceeded through formate and acetate intermediates.

Zhang et al.[17] analyzed Ag particle size effects on PO selectivity over 4 wt % $Ag/BaCO_3$ materials prepared by different techniques. They tested three Ag nanoparticle sizes: ∼20, ∼29, and ∼31 nm. Lower calcination and reduction temperatures helped maintain smaller Ag crystallite sizes, which are more effective for epoxidation of propylene. At 200 °C, they achieved 8.1% propylene conversion at 31.9% PO selectivity.

Guo et al.[18] analyzed the effect of Cu_2O nanoparticle size when the nanoparticles were supported on high-surface-area silica. During propylene oxidation at 300 °C, Cu_2O particles measuring less than 5 nm were the most active, reaching 32.7% propylene conversion, with selectivities for CO_2, acrolein, and PO equal to 34.2, 63.3 and 0.4%, respectively. By an increase in the Cu_2O particle size to 28 nm, the activity drastically dropped: 4.3% propylene conversion under identical reaction conditions. The change in Cu_2O size was reflected less strongly in the selectivity, as CO_2, acrolein, and PO selectivities of 23.9, 72.5 and 0.8% were reported.

The adsorption energy of O_2 on different silver crystalline planes (111, 100, and 110) is low in the range of experimental conditions relevant for propylene epoxidation: 0.1−0.5 bar O_2 partial pressure and 200−400 °C. The Ag surface remains metallic, covered with patches (up to 0.5 monolayer coverage) of different oxygen species.[19] When molecular oxygen (O_2) adsorbs, activates, and dissociates over metals and metal oxides, the following transformation occurs: $O_2 \rightarrow O_2^- \rightarrow 2O^- \rightarrow 2O^{2-}$.[20] The electrophilic character of oxygen species is progressively diminished, thus gradually shifting the tendency from oxygen insertion into the electron-rich C═C bond of propylene toward favoring allylic hydrogen abstraction.

Since silver catalysts have been successfully used to epoxidize ethylene into ethylene oxide ($C_2H_4 + 1/2\ O_2 \rightarrow$ ),[21] they were also a starting point for research in propylene oxidation. It was discovered early on that pure silver preferentially oxidizes the allylic hydrogen, resulting in acrolein as the main reaction product.[22] This is believed to be a consequence of the short lifetime of the selective electrophilic oxygen species and the presence of reactive allylic hydrogen, which is absent in ethylene.[23] As a result, the successful approach of ethylene epoxidation cannot be transferred completely to propylene.

Lu et al.[24] investigated several bulk silver-based catalysts: Ag_2O, AgCl, pure Ag, and Ag modified with several sodium

https://dx.doi.org/10.1021/acscatal.0c03340
ACS Catal. 2020, 10, 13415−13436

and potassium salts (Table 1) at 1 bar and 350 °C. They found that metallic silver is substantially more active than Ag_2O

Table 1. Propylene Epoxidation over Silver Catalysts Modified with Different Promoters[a]

		selectivity (%)			
catalyst	propylene conversion (%)	PO	acetone	aldehyde	acrolein
Ag_2O	12.1	0.2		0.2	0.2
Ag	32.5	0.35	0.4	9.7	0.9
AgCl	0.25				
NaCl/Ag	11.2	29.1	2.1		
NaBr/Ag	2.4	12.1			
KF/Ag	10.7	0.9			
KCl/Ag	6.2				
KBr/Ag	3.5	2.9			

[a]Selectivities are based on carbon mass balance with the difference to 100% being CO_2. Values are reproduced from ref 24. The alkali salt content was 5 wt %.

(Table 1). However, none of the catalysts are selective for PO. This indicates that neither Ag_2O nor metallic Ag is suitable for the epoxidation of propylene. Nevertheless, the 5 wt % NaCl modified Ag catalyst exhibited ∼3-fold lower activity in comparison to pure Ag, but the PO selectivity increased by almost 2 orders of magnitude: from 0.35 to 29.1%. Among potassium-containing salts, the decreasing order of activity F > Cl > Br was obtained on the basis of the anion present, with rgw PO selectivity being very low: between 0 and 2.9%. The authors concluded that NaCl addition triggers the formation of a nanocrystalline AgCl phase, where the chloride changes the electronic properties of the silver catalyst, thus inducing the adsorbed oxygen species to become electrophilic, which is effective for propylene epoxidation.

Farinha Portela et al.[25] tested bulk Cr-doped Ag catalysts and proposed that propylene adsorbs on diatomic oxygen and either desorbs as epoxide or stays bound in an open-chain form. Since total combustion and epoxidation proceed through the same oxametallacycle (OMC) intermediate, the selectivity is independent of the temperature. PO selectivity is, however, negatively influenced by the increasing partial pressure of oxygen in the reaction mixture. The authors suggested that, through an intramolecular hydrogen transfer, hydroperoxides can form, leading to total propylene combustion and loss of PO selectivity.

Lu and Zuo[26] investigated the role of NaCl, $BaCl_2$, LiCl, and NH_4Cl modification of Ag catalysts. The highest improvement in PO yield was achieved by NaCl and $BaCl_2$ modification. With the NaCl-modified Ag catalyst (feed composition 90% air and 10% propylene), 33.4% PO selectivity at 18.6% propylene conversion was achieved at 350 °C (Table 2). A further increase in air concentration led to a significantly lower PO selectivity (10% at 350 °C).

Zemichael et al.[27] investigated the effect of silver metal particle size on propylene oxide selectivity over a $Ag/CaCO_3$ catalyst. The reaction was run with molecular oxygen at atmospheric pressure, and the maximum PO selectivity was achieved at 210 °C. They found that increasing the potassium promoter content (1.7 wt % K) in $Ag/CaCO_3$ catalyst initially slightly decreases the silver particle size (from 70 nm to 20−40 nm). Further increasing the K loading produces a combination of small (∼5 nm) and large (∼100 nm) Ag particles. The

Table 2. Effect of Temperature and Different Chlorine Containing Promoters on the Activity and PO Selectivity of Silver Catalysts[a]

		temp (°C)				
catalyst[b]		250	280	310	350	390
Ag-NaCl	propylene conversion (%)	2.2	4.2	7.8	18.6	29.9
	PO selectivity (%)	51.6	34.5	25	33.4	11.9
Ag-$BaCl_2$	propylene conversion (%)	2.2	3.4	5.3	24.6	30.6
	PO selectivity (%)	0	15.5	19	26.1	14.7
Ag-LiCl	propylene conversion (%)	0	2.3	5.1	8.2	14.1
	PO selectivity (%)	0	0	12.1	27.5	18
Ag-NH_4Cl	propylene conversion (%)	0.8	1.2	2.1	3.2	4.6
	PO selectivity (%)	35.8	17.1	0	0	0

[a]Values are reproduced from ref 26. [b]The concentration of Cl^- in the catalysts was kept constant, and the loading of NaCl in Ag-NaCl was 3.8 wt %.

selectivity for PO passes through a maximum at K loading of 1.7 wt %. The authors suggested that, for optimal PO selectivity, the K-promoted Ag particles should be in the range of 20−40 nm.

To analyze the size effect of silver nanoparticles on PO selectivity, Lei et al.[28] deposited trimeric silver species and ∼3.5 nm particles on amorphous alumina films. On the silver trimers, up to 60 °C, acrolein was the primary reaction product, along with some PO. At 60 °C the onset of total combustion was observed, along with lower acrolein selectivity. Catalysis over 3.5 nm Ag nanoparticles differed noticeably, since PO was the major product up to 130 °C. The normalized activity per surface Ag atom remained very close to that of trimers (∼1 s^{-1}). A DFT analysis revealed that oxygen at the $Ag-Al_2O_3$ interface is not selective. Thus, a decrease in the Ag cluster size increases the fraction of these nonselective interface oxygen species, which leads to allylic hydrogen abstraction and total combustion.

Luo et al.[29] modified bulk silver catalysts with $CuCl_2$, $FeCl_3$, $MnCl_2$, and $AuCl_3$. The catalytic tests were run at atmospheric pressure and 350 °C, with air as the oxidant. Chloride salts decreased the catalytic activity, while they remarkably increased the selectivity to PO (0.42 vs 30.6% for Ag and Ag-$CuCl_2$, respectively). The catalytic activity was strongly dependent on the chloride salt content, and addition of 10 mol % of $CuCl_2$ to Ag led to a significant drop in activity (propylene conversion decreased from 33.2% to 1.85%). However, for optimal PO selectivity, the $Ag/CuCl_2$ molar ratio should be 1/0.5 or above. The authors confirmed the presence of AgCl and CuO in their catalysts, which are both active propylene oxidation catalysts. As a result, the obtained performance cannot be unambiguously attributed to Ag or $CuCl_2$. It was found that the selectivity to PO correlates with the amount of adsorbed oxygen species on the catalyst surface. Thus, the authors suggested that adsorbed oxygen species on the catalyst surface may be the active sites for the epoxidation of propylene.

https://dx.doi.org/10.1021/acscatal.0c03340
ACS Catal. 2020, 10, 13415−13436

In addition to alkali and halide adatoms, modification with several oxides was also found to positively influence PO selectivity over Ag catalysts.

Yao et al.[30] studied the promotional effect of Y_2O_3 on Ag/α-Al_2O_3 catalysts, as well as the effect of support surface area. Over the unmodified Ag/α-Al_2O_3 catalyst, only CO_2 and H_2O were produced. When 0.1 wt % of K_2O was added to the catalyst, the PO selectivity increased to 4.3%, which was further drastically increased (to 46.8%) when Y_2O_3 was added. When the specific surface area of the α-Al_2O_3 support was increased from 0.6 to 10.3 m^2/g and K_2O, Ag, and Y_2O_3 loadings were kept constant, both the activity and selectivity for PO increased about 2-fold. The authors concluded that the role of Y_2O_3 is 2-fold: (i) it decreases the abundance of strongly basic sites created by K_2O without greatly influencing their strength and (ii) it acts as a sintering barrier, preventing the agglomeration of Ag and keeping its size small (~15 nm).

Modification of Ag by MoO_3 was investigated by Jin et al.[31] at a relatively high temperature of 400 °C with a feed comprised of 15.6% C_3H_6, 12.2% O_2, and balance N_2 at 140 kPa total pressure. The optimal MoO_3 content was found to be between 40 and 50 wt % (reaching 35% PO selectivity). XPS analysis of the fresh and spent catalyst revealed the presence of Ag^+ and Mo^{6-x} after reaction. The authors infer that the electron transfer from metallic Ag to MoO_3 leads to Mo having a chemical valence lower than 6+, which coexists together with cationic Ag. This electron donation also increases the basicity of MoO_3. During adsorption of oxygen on the silver surface, electron transfer from silver to adsorbed oxygen makes oxygen take on negative ion properties. The presence of MoO_3 in the catalyst may compete with the adsorbed oxygen for the silver lattice electrons and lead to the reduction of the effective charge transfer to oxygen and thus an increase in the electrophilic property of the adsorbed oxygen species.

The optimal catalyst was further modified with several salts (NaCl, $Ce(NO_3)_3$, $BaCl_2$, or $CsNO_3$). All of them improved PO selectivity (from 34% over bare Ag-MoO_3 to 42−53% with NaCl and $Ce(NO_3)_3$), while also having a minimal negative effect on catalytic activity. Overall, the best-performing catalyst contained 50 wt % of MoO_3 and 2 wt % of NaCl.

Lu et al.[32] synthesized Ag/$CaCO_3$ catalysts modified with alkali- and precious-metal promoters (Table 3). In addition to $CaCO_3$, they tested several other supports such as MgO, CeO_2, γ-Al_2O_3, diamond, and SiC. $CaCO_3$ loaded with 56 wt % Ag showed the highest PO selectivity. Other than PO and acrolein, CO_2 and water were the only reaction products. In general, high-surface-area supports resulted in lower PO selectivity in comparison to those with a lower specific surface area. Among all promoters, only NaCl showed a noticeable increase in PO selectivity, reaching a maximum of 41% at 1 wt % Na loading. NaCl addition had a strong negative effect on the activity of the catalyst: propylene conversion decreased from 60 to 5% after only 0.25 wt % Na addition.

Bere et al.[33] tested the effect of separate feeding of reactants using a tubular membrane reactor with the aim of decreasing the oxygen partial pressure in the reactor and thus improving the PO selectivity. The reaction was run at 240 °C with propylene, N_2, and H_2O fed through the inner (α-alumina) tube, while O_2 and N_2 were fed into the outer stainless steel tube. Water vapor was added to decrease the desorption energy of PO and thus minimize the chance of its further oxidation on the catalyst surface. A catalyst comprised of Ag−Sr bimetallic nanoparticles (Ag/Sr = 10) was impregnated into the pores of the alumina membrane. The highest PO yield of 3.7% was achieved at 6.5% propylene conversion and 57% PO selectivity. When the AgSr loading in the membrane was increased (by up to 5-fold), both the propylene conversion and the PO selectivity decreased. This suggests that smaller bimetallic AgSr clusters are more active and selective for PO in comparison to larger crystallites. In contrast to the high PO selectivity in the membrane reactor, the conventional fixed-bed reactor gave PO yields below 0.5%.

Table 3. Propylene Epoxidation over Silver Catalysts Modified with Different Promoters[a]

catalyst	propylene conversion (%)	selectivity (%)	
		PO	acrolein
Ag(14)−MoO_3(1)/$CaCO_3$	46.3	4.8	0
Ag(56)−Cu(0.04)/$CaCO_3$	41.8	2.5	0
Ag(56)−$Ce(NO_3)_3$(1)/$CaCO_3$	20.8	3.6	0
Ag(56)−$Ba(NO_3)_2$(1)/$CaCO_3$	17.5	4.2	0
Ag(56)−Ir(0.12)/$CaCO_3$	5.1	2.8	0.3
Ag(56)−K_2CO_3(1)/$CaCO_3$	4.4	3.6	0
Ag(14)−K_2CO_3(1)/$CaCO_3$	3.9	3.9	0
Ag(56)−Ir(0.12)/$CaCO_3$[b]	2.9	0	27.9
Ag(14)−$RhCl_3$(1)/$CaCO_3$	1	0	22.7
Ag(56)−NaCl(1)/$CaCO_3$	1.4	39.2	0
Ag(56)−NaCl(1)/$CaCO_3$(5)−α-Al_2O_3	3.3	30.4	0
Ag(56)−NaCl(1)/α-Al_2O_3	4.4	30.1	0
Ag(56)−KCl(1)/$CaCO_3$	1.4	15.3	0
Ag(56)−NaCl(1)/CeO_2	3.2	13.4	0
Ag(14)−NaCl(1)/$CaCO_3$	1.6	7.5	0
Ag(56)−NaCl(1)/SiC	1.7	5.2	0

[a]Values are reproduced from ref 32. [b]Prior to the reaction, the catalyst was reduced in 20 mol % H_2 in He at 350 °C for 2 h; catalytic tests were performed at 260 °C.

Triwahyono et al.[34] analyzed the epoxidation of propylene in a microporous glass (MPG) membrane reactor containing immobilized cesium−silver (Cs−Ag) catalysts. For a quantitative evaluation of the membrane reactor efficiency in producing PO, three different reactor configurations were compared: a diffusion flow reactor (DFR), a convection flow reactor (CFR), and a plug flow reactor (PFR). At 250 °C, PO selectivities of 13 and 17% were attained in CFR and DFR reactor configurations, in comparison to 2% in a *conventional* PFR mode. Increasing the total flow rate had a positive effect on PO selectivity. The PO selectivity improvement achieved in the membrane reactors was attributed to a shortening of PO residence time over the catalyst, thus minimizing the further oxidation of PO. A simulation of the convection-flow membrane reactor efficiency by Golman et al.[35] demonstrated that the convection flow in the pores of a membrane has a strong positive influence on the selectivity of the intermediate for the sequential reaction A → B → C. The convection flow in the pores of the membrane shortens the residence time of PO, and the hydrodynamic effect of this type of flow accelerates the removal of the heat generated by the exothermic reaction. The same authors also performed a steady-state kinetic analysis of their convective flow membrane reactor. Their calculations were in good agreement with the L-H model, where the equations were based on two active adsorption sites for the synthesis of PO and a competitive adsorption on a single site for deep oxidation of propylene to CO_2.

https://dx.doi.org/10.1021/acscatal.0c03340
ACS Catal. 2020, 10, 13415−13436

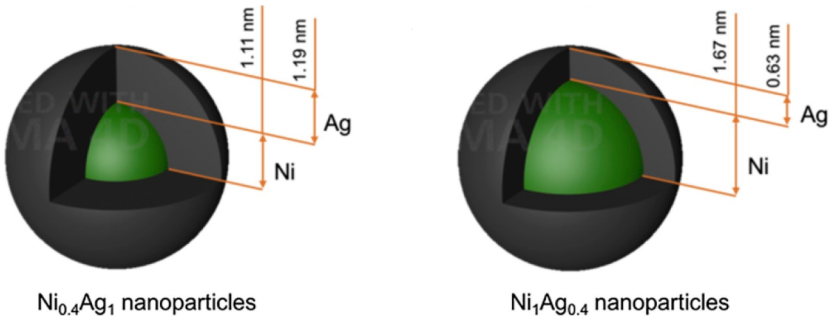

Figure 3. Schematic representation of Ni−Ag core−shell catalysts used by Yu et al. Reproduced with permission from ref 43. Copyright 2018, Elsevier.

Hazbun[36] reported a PO selectivity in excess of 30% with a propylene conversion between 10 and 15%, when the epoxidation reaction was run between 300 and 500 °C in an oxygen-permeable tubular membrane reactor made of ZrO_2−Y_2O_3−TiO_2, containing 8 wt % Ag catalyst, promoted by calcium and barium.

The patent literature also reveals that the PO selectivity can be increased notably over silver-based catalysts by cofeeding low concentrations (up to 2000 ppm) of nitrogen oxides (such as NO), aliphatic halides (20−500 ppm) such as ethyl chloride, and substantial amounts of CO_2 (5−25 vol %) in addition to oxygen and propylene. For example, a calcium carbonate support containing 40 wt % Ag promoted by 2 wt % K and 4.7 wt % W in the absence of cofed CO_2 achieved 41% PO selectivity at 13% propylene conversion, whereas cofeeding 10 vol % CO_2 resulted in 54% PO selectivity at 10% propylene conversion.[37] No explanation of the role of CO_2 was provided. The role of cofeeding gaseous aliphatic halide is to keep the most active sites deactivated, thus preventing the deep oxidation of propene.[38] Chloride is known to leach from Ag-based catalysts during epoxidation.[39]

Zheng et al.[40] modified the 3% Ag/$BaCO_3$ with Cu. The PO selectivity strongly depends on the Ag/Cu ratio, and the highest PO selectivity (55% at 3.6% propylene conversion) was reached for a Ag/Cu ratio of 95/5. Pure Ag/$BaCO_3$ and Cu/$BaCO_3$ achieved 10 and 5% PO selectivities, respectively. A stability test showed that, after 6 h of time on stream (TOS), the catalyst retained only ∼40% of initial activity; however, the PO selectivity remained stable. This suggests that only the total number of active sites, and not their nature, changed during catalyst deactivation. Fouling of active sites by adsorption of hydrocarbons was identified as the reason for deactivation, which could be regenerated by heating the catalyst in N_2 to 450 °C. The role of Cu, identified through XRD and TEM analyses, was to effectively regulate the size of Ag crystallites by restraining their agglomeration. XPS results indicate that the presence of Cu can withdraw electrons from an adjacent Ag, giving it a cationic character. This is beneficial to produce active sites where (selective) electrophilic oxygen species can be stabilized.

Ghosh et al.[41] tested Ag supported on Cr_2O_3, MoO_3, and WO_3. The Ag/WO_3 catalyst containing highly dispersed silver nanoparticles (2−5 nm) on WO_3 nanorods outperformed them all. In contrast to the majority of propylene epoxidation work in the literature that was performed at ∼1 bar, these authors investigated the effect of reaction pressure on PO selectivity. At a total pressure of 1 MPa, the propylene conversion was ∼7% and the PO selectivity was 39%. Increasing the total pressure significantly improved the PO yield: at 3−4 MPa, the propylene conversion reached ∼25% and PO selectivity 55%. Increasing the temperature from 200 to 400 °C caused the propylene conversion to increase (from 9% to 27%) but was accompanied by a drop in PO selectivity (from 91% to 54%). The optimal reaction conditions were 250 °C and 2 MPa total pressure.

Huš and Hellman[19] using DFT calculations observed a change in the epoxidation mechanism at elevated pressures, albeit this was calculated for ethylene epoxidation. The origin of the mechanism shift was traced to the equilibrium surface coverage. In all instances, O* is the only species with a non-negligible coverage of the catalyst. With increasing pressure, the O* coverage is also increasing up to 0.02 bar, at which point the trend reverses. It appears that, at this point, the partial pressure of ethylene becomes large enough to react more quickly with the surface oxygen. As a result, the surface population with oxygen species decreases at elevated pressures, resulting in higher epoxide selectivity.

Lee et al.[42] investigated the effect of 20Ag/ZrO_2 catalyst modification by Mo (0−5 wt %) and W (0−5 wt %). An XPS analysis showed an increase in binding energy of the Ag $3d_{5/2}$ band on simultaneous modification by Mo and W, indicating electron transfer from metallic silver to adjacent molybdenum and tungsten oxides and a change of the metallic character of silver to cationic. Consequentially, this leads to a decelerated electron flow from silver to adsorbed oxygen, thus slowing down its activation. When a promoter which attracts electrons from silver is present, the nucleophilicity of molecular oxygen adsorbed on the silver surface is reduced, leading to a suppressed total oxidation of propylene. Catalytic tests revealed a remarkable correlation between PO selectivity with a red shift in the Ag $3d_{5/2}$ binding energy. The optimal catalyst (20Ag-3.75Mo-1.25W/ZrO_2) enabled 12.5% propylene conversion and 60% PO selectivity at 460 °C.

Yu et al.[14] synthesized Ag nanocubes and nanospheres which expose predominantly (100) and (111) crystalline planes and dispersed them over several oxide supports (La_2O_3, Gd_2O_3, Eu_2O_3, Yb_2O_3, Lu_2O_3, and Al_2O_3). Independently, the Ag nanoshaped particles or individual oxide supports do not yield any PO. Their interfaces, on the other hand, such as Ag nanocubes/La_2O_3, can achieve a propylene conversion of 11.6% with a PO selectivity of 51% at 1 bar and 270 °C. The DFT calculations revealed that the polar surface of La_2O_3 decomposes molecular oxygen, which then migrates to the Ag(100) plane of the nanocubes. The lower combustion and AHS rates are likely due to longer interatomic distances of the Ag(100) surface in comparison to Ag(111), which decelerates

https://dx.doi.org/10.1021/acscatal.0c03340
ACS Catal. 2020, 10, 13415−13436

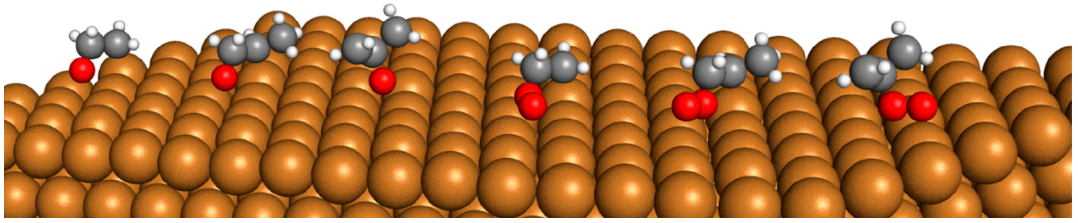

Figure 4. All possible oxametallacyles (OMC) in ethylene and propylene epoxidation on Cu(111). From left to right: OME, OMP1, OMP2, OOME, OOMP1, OOMP2. Only one possible adsorption mode is shown. Structures on silver catalysts are analogous.

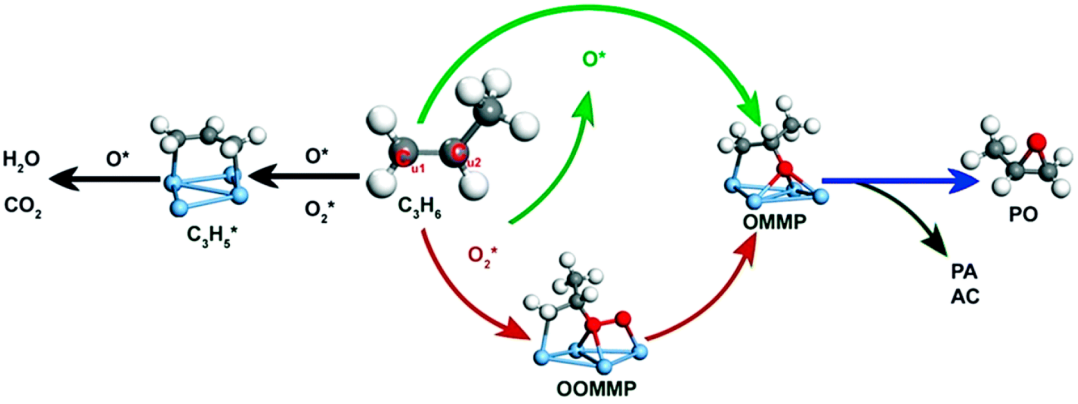

Figure 5. Reaction scheme of propylene oxidation by monatomic and diatomic oxygen proposed by Dai et al. Reproduced with permission from ref 50. Copyright 2017, Royal Society of Chemistry.

the reaction of adsorbed oxygen with the allylic hydrogen. The authors conclude that the Ag/La_2O_3 interface is the active perimeter and a support that contains a high fraction of mobile surface oxygen species is a prerequisite for high PO selectivity.

Similarly, modification of the Ag−Ag interatomic distances was achieved in core−shell Ag@Ni/SBA-15 catalysts (Figure 3), according to an EXAFS analysis by Yu et al.[43] Their results indicate that Ni is in the core of the nanoparticles, which are encapsulated by a ∼1 nm thin layer of Ag atoms. With an optimal nickel to silver ratio ($Ni_1Ag_{0.4}$), the core−shell catalysts exhibited excellent stability after 10 h of TOS with a PO selectivity of ∼70% at a propylene conversion under 1%.

To summarize, single-crystal studies are very useful for establishing structure−activity−selectivity relationships of different silver facets for propylene oxidation. These studies identified the Ag(100) facet as the most selective for PO. However, the reactions are often performed in UHV or as temperature-programmed desorption studies with only propylene in the gas phase. Experimental evidence with unsupported shaped Ag nanocrystals, exposing the most selective (100) facets under relevant reaction conditions (0.1−0.5 bar O_2 and C_3H_6 partial pressure and 200−400 °C) is lacking, which would confirm the transferability of single-crystal catalytic performance into more practical applications.[14] More abundant data with polycrystalline bulk silver powders (exposing mainly Ag(111) facet), however, give information on the PO selectivity dependence on particle size. Upon the fixation of polycrystalline Ag nanoparticles over different supports, their activity and selectivity are drastically changed, due to several possible contributions: electron withdrawal or donation as a result of the basicity and acidity of the support, the intrinsic activity of the support or interfacial Ag−O−support sites for O_2 activation,[28,44] and a change of Ag−Ag interatomic distances.[43] Despite being crucial for understanding the structure−activity−selectivity dependence of propylene epoxidation over silver, the results obtained over single-crystal and unsupported Ag metal nanopowders do not necessarily convey the performance of catalysts where metal nanoparticles are supported. The latter, however, are of higher practical and industrial interest.

2.1. Theoretical DFT Analysis of Silver-Based Catalysts in Propylene Epoxidation. In selective propylene (and ethylene) oxidation, the reaction intermediates responsible for the production of epoxide are oxametallacycles (OMC), which is a generic term for structures where activated surface oxygen is bound to an sp^2-hybridized carbon atom before further rearrangements or transformations. As both carbon atoms in ethylene are equivalent, one oxametallacycle can form with ethylene (OME: oxygen−metal−ethylene). In propylene, the sp^2 carbon atoms are inequivalent, giving rise to two possible oxametallacycles (OMP1 and OMP2) with atomic oxygen and two more ("dioxametallacycles": OOMP1 or OOMP2) with molecular oxygen, which can form on oxides,[45] metallic surfaces,[46] or partially metallic surfaces.[47] Analogously, an ethylene oxametallacycle with molecular oxygen (OOME) could also be possible, but it has not yet been observed.

Figure 4 gives some possible structures. Some authors further distinguish between OME and OMME,[48] OMP1 and OMMP1, and OMP2 and OMMP2 on account of how they bind to the surface,[49] which is especially relevant on less densely packed surfaces, such as 110. Analogously, OOMP1 and OOMMP1 and OOMP2 and OOMMP2 can be distinguished.[50]

The consensus in the scientific community is that, for PO selectivity, the oxametallacycle (OMC) is the prerequisite reaction intermediate.[46−56] In the following section, the formation and different desorption possibilities of oxametallacycle intermediates are discussed. DFT studies have been used extensively to both discover the reaction mechanism and to evaluate the energetics and kinetics of its individual steps. In

https://dx.doi.org/10.1021/acscatal.0c03340
ACS Catal. 2020, 10, 13415−13436

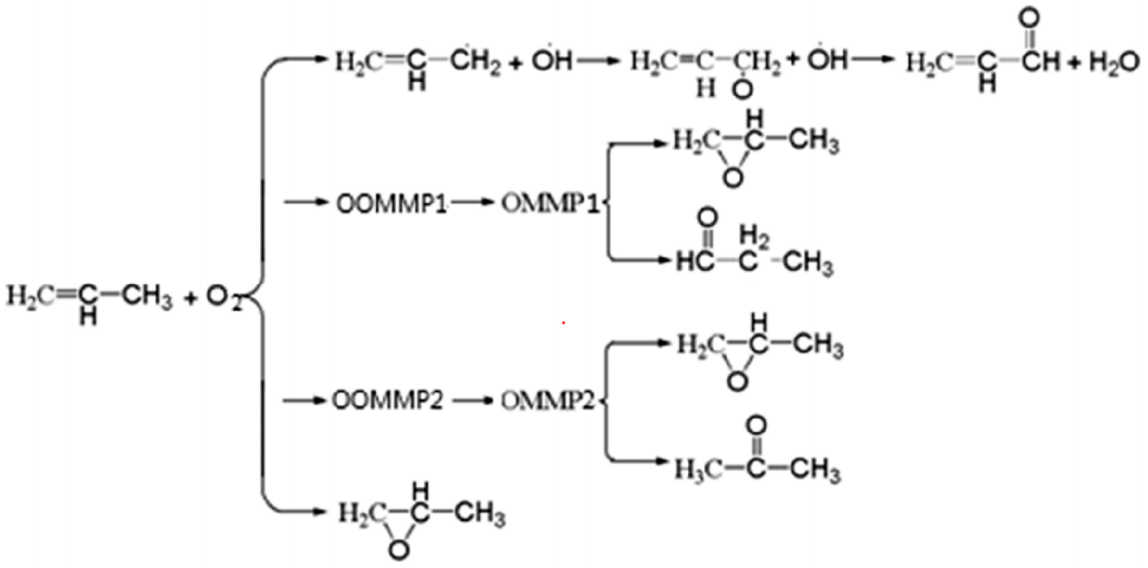

Figure 6. Proposed reaction pathways for propylene selective oxidation on Ag(111) as proposed by Zhao and Wang. Reproduced with permission from ref 46. Copyright 2019, American Chemical Society.

the case of ethylene, the mechanism is simple on the account of the symmetrical nature of the molecule. Ethylene reacts with an adsorbed oxygen atom, forming an oxametallacycle (OMC, also called OMME), which can convert to an epoxide (EO) or acetaldehyde (AA). Alternatively, a sufficiently nucleophilic oxygen atom can cleave off the vinylic hydrogen from ethylene. While lumped reaction models include subsequent oxidation reactions to CO_2, pure DFT models do not because these reactions do not influence the selectivity.[57]

In the case of propylene, the reaction space is larger. Propylene can react with an adsorbed oxygen atom in three ways: it can form an oxametallacycle through either of its sp^2-hybridized carbon atoms (in general OMC, distinguished into OMMP1 and OMMP2) or it can have its allylic hydrogen stripped off (AHS). In the latter case, a second hydrogen stripping and addition of oxygen yield acrolein. OMMP1 can transform into PO or undergo a hydrogen migration, yielding propanal. Similarly, OMMP2 can form PO or acetone. It is also possible for propylene to react directly with molecular oxygen, forming OOMMP1 and OOMMP2,[50] which transform into OMMP1 and OMMP2 (Figure 5). On other catalysts, such as RuO_2(110), a direct insertion of a surface oxygen atom into the propylene double bond to yield PO is also possible.[49]

DFT studies on metallic Cu(111) and Ag(111) surfaces[58] have shown that propylene orientation upon adsorption is an important factor in PO selectivity. On Ag(111), propylene can adsorb in four distinct configurations relative to the oxygen adatom. The energetics of the configurations differ by less than 0.08 eV, meaning all will be kinetically accessible during experiments. Depending on the configuration attained, the OMMP1 or AHS path is followed, while OMMP2 was ruled out on the basis of an overly high activation barrier. The barriers for the conversion of OMMP1 into PO and propanal are comparable (0.62 and 0.56 eV, respectively), meaning that the reaction will be poorly selective. On Cu(111), the abstraction of an allylic hydrogen atom and OMMP1 formation have similar barriers (0.60 and 0.54 eV, respectively), while OMMP2 is kinetically inaccessible. OMMP1 more readily converts into PO (a barrier of 0.96 eV) in comparison to propanal (1.10 eV). Using the rate constants estimated from the transition-state theory, on Ag(111) around 99% of propylene molecules are predicted to undergo allylic hydrogen stripping (AHS). On Cu(111) the situation is very different, and the predicted PO selectivity is over 50%. This significant difference was attributed to the lower basicity of oxygen (more electrophilic) on a Cu(111) surface in comparison to Ag(111), thus inhibiting AHS.

Dai et al.[50] investigated the reaction on Au (111), Cu (111), and Ag (111, 211, and 100). They noted that, when adsorbed molecular oxygen (O_2) is used, the reaction barrier for the formation of OMMP (through OOMMP) is lower than for AHS. When monatomic oxygen adatoms (O^{2-} or O^-) were used, AHS was favored in comparison to the formation of OMMP. Additionally, a good correlation was found between allylic hydrogen affinity for the oxidizing agent (monatomic vs diatomic oxygen) and the reaction barrier for AHS. The beneficial effect of O_2 was consistent across all investigated surfaces, extended (111) and stepped (110, 211). When O_2 is the oxidant, OOMMP2 is formed, which then converts into OMMP2 following the cleavage of the O−O bond. A higher selectivity for OMMP formation when molecular oxygen is used can improve the overall selectivity for PO to possibly reach 90%. However, this is dependent on the prevention of O_2 dissociation, which could be brought about by surface modifications, halogen doping, alloy fabrications, and reaction condition manipulation.

Zhao and Wang[46] investigated how alkali (Na and K) and Cl promoters affect the propylene oxidation pathways on Ag(111) and improve selectivity. The promoter atoms were modeled as adatoms. The authors found that Na and K stabilize the binding of O_2 on the surface by increasing the electron density, while Cl has a small inhibitory effect on O_2 adsorption. The effect on the adsorption of propylene and other adsorbates in negligible. Focusing on the formation of OOMMP2 by O_2 on the basis of thermodynamic considerations, the authors showed that alkali doping increases the activation barrier for the primary chemistry reactions (AHS or O(O)MMP2 formation) and as well as secondary reactions (OMMP2 conversion to PO or acetone). Cl, however, increases the activation energy of the AHS step and reduces the activation

https://dx.doi.org/10.1021/acscatal.0c03340
ACS Catal. 2020, 10, 13415−13436

energy of OOMMP2 formation, as well as of the PO or acetone desorption steps (Figure 6). Although all barriers are increased, their *difference* (defined as ΔE_a(primary) = E_a(AHS) − E_a(OMC) and ΔE_a(secondary) = E_a(AC) − E_a(PO)) is crucial for selectivity and becomes more favorable upon doping. Thus, Na and K on Ag(111) can improve the PO selectivity through the secondary chemistry (PO formation is favored over acetone formation), whereas Cl can simultaneously improve the reaction selectivity of the primary (OOMMP2 formation) and secondary chemistry (Figure 7).

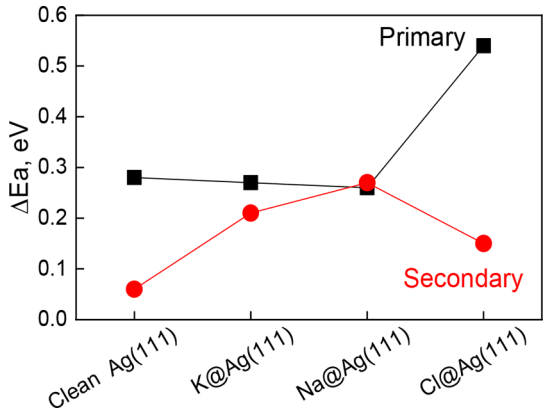

Figure 7. Variation of ΔE_a for primary and secondary chemistry with different additives on a Ag(111) surface. ΔE_a(primary) = E_a(AHS) − E_a(OMC); ΔE_a(secondary) = E_a(AC) − E_a(PO). Redrawn from data published by Zhao and Wang.[46]

Pulido et al.[12] investigated direct propylene epoxidation over Ag(100) and Ag(111) with atomic oxygen. On a clean Ag(100) surface, oxygen atoms occupy the hollow sites, coordinated with four Ag atoms, whereas on a Ag(111) surface, the most stable site is on 3-fold-coordinated *fcc* hollow sites. This results in much smaller Ag−O interaction energies on Ag(111), in comparison to Ag(100). O_2 binds more strongly to Ag(100) than to Ag(111) with adsorption energies of −65 and −21 kJ mol^{-1}, respectively. The activation barrier for oxygen dissociation is also greater on Ag(111) by 20 kJ mol^{-1} in comparison to Ag(100). On Ag(100), the barrier for AHS is merely 29 kJ mol^{-1} (0.3 eV), while for the formation of OMMP1 and OMMP2, the barriers are 59 and 48 kJ mol^{-1}, respectively, indicating that no PO will be formed. On Ag(111), the barrier for AHS (33 kJ mol^{-1}), again, is lower than that for the formation of OMMP2 (52 kJ mol^{-1}). Thus, total oxidation is the preferred pathway regardless of the terminating crystal plane. The rate-determining step is the dissociation of oxygen. However, calculations predict that PO and other oxygenates could be produced with higher selectivity on the Ag(100) surface. The calculations were supported by catalytic tests, which confirmed the predicted selectivity trends.

Lei at al.[28] supplemented their experimental work on alumina-supported Ag_3 clusters with theoretical calculations. They modeled an Ag_3 cluster adsorbed on a (010) γ-alumina surface. The barrier for oxygen dissociation is 0.49 eV, which is much lower than that on Ag(111). Upon adsorption, propylene reacts with oxygen to form an oxametallacycle (E_a = 0.84 eV) and ultimately PO (E_a = 0.80 eV). The pathways occurring from the oxametallacycle leading to acrolein, CO_2, and propanal are unfavorable. The AHS route has a low activation barrier (E_a = 0.53 eV for the first stripping) and yields combustion products.

Cheng et al. studied the reaction on alumina-supported silver aggregates, both experimentally and theoretically.[59] For theoretical studies, Ag_{19} and Ag_{20} clusters, truncated from the Ag bulk, were used because 3 nm aggregates are computationally prohibitive. The clusters have similar geometries, consisting of pyramid-like and hexagon-like facets and corner and edge sites. However, they differ in their electronic structure: Ag_{19} has one unpaired electron while Ag_{20} has none, which has some effect on the reaction thermodynamics and kinetics. On Ag_{19}, oxygen dissociation proceeds on the pentagonal-pyramidal neighboring site (*E*a = 0.46 eV), while on Ag_{20} it proceeds on the hexagonal facet (E_a = 0.66 eV). This is a consequence of a curve crossing from the triplet to the singlet state on Ag_{20}, which is not present on Ag_{19}. For the epoxidation reaction, however, the difference between Ag_{19} and Ag_{20} is negligible, as the spin is well delocalized on the cluster. The adsorption energy of propylene is −0.50 eV, and the barrier for conversion to OMMP2 is around 0.57 eV. The subsequent barriers for the formation of PO are 1.06 and 1.28 eV on Ag_{19} and Ag_{20}, respectively. On alumina-supported Ag_{19}, the barrier for oxygen dissociation remains similar (0.52 eV). However, the energetics for epoxidation by the interfacial oxygen atom is changed. The barrier for the formation of OMMP2 is lowered to 0.38 eV and that for the formation of PO to 0.51 eV. Surprisingly, although AHS is found to be even more favorable on supported Ag_{19} with an activation barrier as low as 0.05 eV, experimentally some PO was observed. The authors ascribe this discrepancy to the fact that, for acrolein production, oxygen availability might be a limiting factor.

Feng et al. studied the reaction on Au but also included a case where one surface Au atom was substituted with Ag. They found that the introduction of Ag affects the electronic properties of Au and improves the O_2 adsorption by increasing the net charge of adsorbed O_2.[60]

While most studies have dealt with metallic silver catalysts, Tezsevin et al. focused on Ag_2O(001).[61] They studied the pristine surface and a modified structure with one O vacancy. PO can form on both surfaces, and its production is limited by the desorption rate. On the pristine surface, the formation of OMMP1, OMMP2, PO (by a one-step direct insertion), and the AHS all proceed barrierlessly. Among those, PO is thermodynamically the most stable. Even when OMMP1 or OMMP2 form, the barriers for their conversion to PO are lower (<0.1 eV) than those for the conversion to propanal (0.2 eV) or acetone (0.3 eV), respectively. On the surface with an oxygen vacancy, the formation of OMMP1 and OMMP2 is less favorable than a direct formation of PO, although all steps *do* have barriers.

Fellah and Onal used a [$Ag_{14}O_9$] cluster as a model for the Ag_2O(001) surface[62] and showed that the AHS pathway competes with the PO-producing route. The barrier for the allylic stripping was 38 kJ mol^{-1}, and those for propylene adsorption were 34 and 38 kJ mol^{-1}, depending on the adsorption mode. The adsorption of propylene on this surface is activated, as propyleneoxy intermediates are immediately formed. Oxametallacycle intermediates were not observed, which is ascribed to the lower basicity of surface oxygen in Ag_2O. Upon adsorption, PO is formed via the C1 or C2 route (barriers of 71 and 84 kJ mol^{-1}) and not propanal (176 kJ mol^{-1}) or acetone (164 kJ mol^{-1}).

https://dx.doi.org/10.1021/acscatal.0c03340
ACS Catal. 2020, 10, 13415−13436

Table 4. Propylene Conversion and Selectivity at Different Reaction Temperatures over CuO_x/SBA-15 and K^+-CuO_x/SBA-15 Catalysts[a]

			selectivity (%)				
catalyst[b]	temp (°C)	C_3H_6 conversion (%)	PO	acrolein	others[c]	CO	CO_2
CuO_x/SBA-15	225	0.8	6.9	41	16	11	25
	250	2.7	4.1	25	6	14	51
	275	6.6	1.8	21	2.9	18	56
	300	14	0.6	17	1.3	20	62
	350	33	0.1	12	0.8	26	61
K^+-CuO_x/SBA-15	225	0.4	59	8.7	3.5	4.2	24
	250	1	46	6.4	1.9	5.5	40
	275	2.1	35	4.9	1.1	9.1	49
	300	4.7	26	4	0.7	10	60
	325	7.2	20	3.4	0.5	13	63
	350	13	14	2.9	0.3	16	67

[a]Values are reproduced from ref 81. Reaction conditions: catalyst mass 0.20 g; partial pressures of C_3H_6 and O_2 2.5 and 98.8 kPa, respectively; total flow rate 60 mL min^{-1}. [b]Copper content, 1.0 wt %; K/Cu = 0.70. [c]Allyl alcohol, acetone, and acetaldehyde.

3. EXPERIMENTAL PROPYLENE EPOXIDATION ON COPPER-BASED CATALYSTS

Copper has been extensively tested in propylene oxidation with molecular oxygen. Early studies were focused more on acrolein reaction pathways,[63−68] whereas PO was rarely mentioned as the main product.[69−72] Only upon alkali or chlorine modification does substantial PO selectivity arise.

Under propylene epoxidation conditions (200−400 °C, $P(O_2)$ = 0.01−0.5 bar, $P(C_3H_6)$ = 0.01−0.5 bar), copper is present predominantly as Cu_2O in coexistence with CuO.[73−76] As a result, epoxidation can occur through the Mars−van Krevelen (MvK) or Langmuir−Hinshelwood (LH) mechanism. This is the first and fundamental difference in comparison to Ag-based catalysts, which remain metallic during propylene epoxidation and where the Langmuir−Hinshelwood mechanism should prevail.

Single-crystal studies of propylene oxidation over Cu_2O-(100) and (111) facets were performed by and Schulz and Cox.[77,78] Reitz and Solomon[79] investigated propylene oxidation on the Cu(111) facet, which was oxidized to Cu_2O and CuO. Their XPS studies showed that, below 473 K, the adsorbed surface species over Cu_2O(111) are tentatively assigned as allyl alkoxides, whereas between 523 and 623 K, they change to aldehyde or ketone groups. However, on CuO(111), the aldehydic or carboxylate species are observed already at 350 K, identifying the CuO surface as more reactive toward deep propylene oxidation, in comparison to Cu_2O.

In comparing propylene adsorption on Cu_2O(100) and (111), Schulz and Cox[77] discovered notable differences between both surfaces, with propene dissociation to allyl (C_3H_5) species over Cu_2O(111). Desorption of propene caused the formation of surface oxygen vacancies and CO as the only desorption product. Once the oxygen-deficient surface was formed, the propene desorption shifted to a higher temperature, indicating a stronger binding of propene to the oxygen-deficient sites.

The same authors in a later study[78] investigated the interaction between propylene and a Cu^+-terminated Cu_2O-(100) facet, an oxygen-terminated Cu_2O(100) facet, and a Cu_2O (111) facet with accessible Cu and O sites using XPS and temperature-programmed desorption techniques. Clear structure sensitivity of the propylene interaction with Cu_2O was observed, on the basis of the temperature of propylene desorption from the probed surface. Propylene dissociation at 300 K does not appear to depend on the exposed sites on Cu_2O. The oxidation to acrolein is promoted by coordinatively unsaturated surface oxygen, as present on the Cu_2O(111) surface. The two-coordinated surface oxygen on the oxygen-terminated (100) surface was found to promote nonselective complete oxidation, and both partial and total oxidation products are formed from the lattice oxygen. In no case was PO observed as a reaction product.

Hua et al.[11] investigated the crystal-plane-controlled selectivity of Cu_2O in propylene oxidation. They synthesized nanoshaped Cu_2O crystals exposing different facets: octahedra, (111); rhombic dodecahedra, (110); cubes, (100). Propylene oxide, acrolein, and CO_2 were identified as the reaction products. With the combination of catalytic tests and XPS, TEM, DRIFTS, and DFT techniques, they arrived at the conclusion that one-coordinated Cu on Cu_2O(111), three-coordinated O on Cu_2O(110), and two-coordinated O on Cu_2O(100) were the catalytically active sites for the production of acrolein, propylene oxide, and CO_2, respectively. The highest PO selectivity was 20% on Cu_2O (110), making crystal-plane engineering of Cu_2O a useful strategy for developing PO-selective catalysts.

Su et al.[80] studied the effect of nanoparticle size of unsupported copper oxide in direct propylene epoxidation. They found that in the size range between 25 and 58 nm, there is an optimum at 41 nm. They found that the catalysts contain a mixture of Cu^+ and Cu^0, and varying the calcination temperature between 200 and 500 °C did not affect the ratio between the two oxidation states, only the crystallite size. They proposed that the smaller particles have a larger fraction of step and kink sites, which are the sites of nucleophilic oxygen, promoting AHS. Reducing the copper oxide phase completely by H_2 pretreatment completely destroyed PO selectivity and increased the Cu particle size to 160 nm. Consistent with other research, the authors also confirmed that increasing the temperature drastically increases CO_2 selectivity at the expense of PO selectivity.

Wang et al.[81] tested 1 wt % copper dispersed over ordered mesoporous silica (SBA-15), modified with different alkali and alkaline-earth salts. Modification with alkali metals decreased the activity and increased the PO selectivity in the trend Li <

https://dx.doi.org/10.1021/acscatal.0c03340
ACS Catal. 2020, 10, 13415−13436

Na < K < Rb < Cs, while alkali-earth metals had a minimal effect on both activity and PO selectivity. The highest PO yield (up to 14%, depending on reaction temperature) was achieved after modification with potassium, identifying it is as a most suitable promoter at an optimal K/Cu ratio of 0.7 (Table 4). Among several potassium precursors (KAc, KOH, KCl, and K_2CO_3), acetate gave the highest PO yields. H_2-TPR, NH_3-TPD, and UV−vis analyses confirmed a direct interaction between CuO_x and K^+, where both the strength and the amount of acid sites decreased in comparison to pristine CuO_x/SiO_2 catalyst. This contributes to higher PO selectivity, since there is less chance for it to undergo isomerization and further oxidation to CO_x over acidic sites. Also, modification with K^+ produced smaller CuO_x clusters and reactivity of lattice oxygen associated with CuO_x clusters or Cu^{2+} ions was suppressed. The working catalyst contains a combination of Cu_2O and CuO phases.

Wang et al.[82] investigated the mechanism of the promotional effect of Cl^- on Cu_2O nanocubes in the direct epoxidation of propylene. The synthesized nanocubes exposed (100) surface planes. Similarly to the findings of Teržan et al.,[73] they reported that a less nucleophilic oxygen is the key for high propylene selectivity. In the absence of Cl^-, the surface oxygen remained nucleophilic and initiated hydrogen abstraction. They also found that the selectivity and conversion exhibit a volcano-type correlation. The latter is reduced as the chloride coverage is increased, since there is a limited interaction between surface oxygen and propylene. The optimal loading, giving the highest TOF, was found to be 0.33 wt % of NH_4Cl.

Vaughan et al.[83] tested Cu/SiO_2 catalysts containing 1 and 5 wt % Cu in propylene epoxidation. The 1% Cu/SiO_2 achieved up to 53% PO selectivity at 225 °C, whereas PO selectivity maxed out at 17% for 5% the Cu/SiO_2 sample. Control tests at 225 °C confirmed that in either the presence or absence of oxygen, PO isomerizes to propanal, which can undergo dehydrogenation to acrolein. Promotion of the Cu/SiO_2 catalysts by NaCl or Cl^- actually had a detrimental effect on PO selectivity. The authors used XRD and XPS techniques to analyze the selective catalyst after the reaction and concluded that the active phase for PO formation is a highly dispersed form of metallic copper. The last two conclusions contradict to many recent reports employing *in situ* characterization (*vide infra*). This could, however, be related to the relatively low reaction temperature, which is insufficient for copper oxidation and which results in a different action of the alkali and halide promoter.

He et al.[84] synthesized a 5 wt % CuO_x/SiO_2 catalyst and modified it with alkali metals (Li, Na, K, Rb, and Cs). The catalytic activity was decreased by about 50% in comparison to the pristine sample, whereas PO selectivity increased from 10 to 20 times. Cesium was the optimal promoter with a Cs/Cu molar ratio of 0.4. Prolonging the residence time decreased the selectivity for PO and acrolein and increased the selectivity for CO_x, indicating that both oxygenates can easily be oxidized further. The Cs^+ modification inhibits isomerization of PO by lowering the total acidity of the catalyst. Injecting propylene pulses over CuO_x/SiO_2 and Cs-modified CuO_x/SiO_2 catalyst produced acrolein with 75−97% selectivity, with CO_x making up the difference to complete carbon mass balance. This clearly revealed lattice oxygen as the nonselective oxygen species. The authors observed that regardless if the catalyst was reduced prior to catalytic tests (copper phase was converted to a mixture of Cu^0 and Cu^+), or oxidized with oxygen (only Cu^{2+} was present), a mixture of Cu^+ and Cu^{2+} is present during propylene epoxidation. The Cu^+ generated during the reaction functions as the selective epoxidation site, where molecular oxygen is activated (Figure 8). The presence of Cs^+ not only inhibits the consecutive conversion of PO but also decreases the reactivity of the lattice oxygen, contributing to a higher PO selectivity.

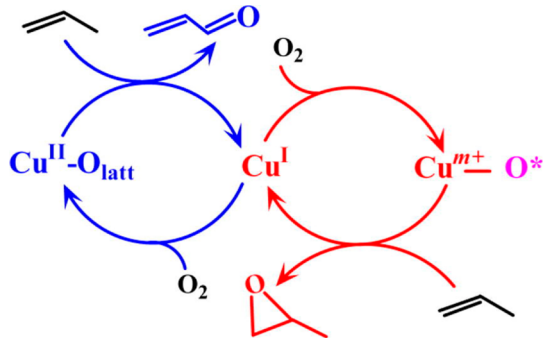

Figure 8. Reaction pathways producing different products with the participation of lattice or surface chemisorbed oxygen species over CuO_x/SiO_2 catalysts, as proposed by He et al. Reproduced with permission from ref 84. Copyright 2012, Elsevier.

Marimuthu et al.[74] studied ∼40 nm Cu nanoparticles supported on amorphous silica for propylene epoxidation. They found that, under purely thermocatalytic conditions, the selectivity for propylene oxide remained below 20%. The copper nanoparticles were immediately oxidized and formed a Cu_2O shell over the metallic copper core, revealing Cu^+ as the working oxidation state of the catalyst at 250 °C. Under photothermal reaction conditions when the catalyst was excited by visible light, the PO selectivity increased ∼2.5-fold. The sudden rise in PO selectivity was attributed to a reduction of the Cu_2O shell on the nanoparticles and its conversion into purely metallic copper. During combined photothermocatalytic experiments, an increase in CO_2 selectivity as a result of total combustion of propylene oxygenates was also observed. It should be noted that the epoxidation mechanisms under plasmonic and thermocatalytic modes of operation are different, generally due to an additional plasmon-driven pathway of molecular oxygen activation.

Yang et al.[85] synthesized $TiCuO_x$ on a Cu(111) surface with the aim of stabilizing copper in the Cu^+ oxidation state. With high-resolution electron energy loss spectroscopy (HR-EELS) and DFT analysis, they confirmed the presence of the propylene oxametallacycle on $TiCuO_x$. The signals assigned to OMC binding were not observed on either Cu(111) or Cu_2O. From the temperature-programmed desorption (TPD) of the catalyst saturated with propylene and O_2, a PO selectivity of 69% was obtained. The Cu^+ in the $TiCuO_x$ phase was not reduced, which indicates a lessened reactivity of the lattice oxygen species in comparison to Cu_2O. The combined TPD, XPS, and HR-EELS analyses showed that PO chemisorbs on the surface of $TiCuO_x$. More importantly, it desorbs as propylene oxide and no isomerization takes place. This is not the case over Cu(111) or Cu_2O, thus revealing the importance of the Cu−Ti interface.

Song and Wang[45] used DFT analysis to study the preference of different oxygen species (O^{2-}, O^-, and O_2^-) found on the $Cu_2O(111)$ surface for either AHS or epoxidation (Figure 9). The most active species (lowest activation barriers) is the

https://dx.doi.org/10.1021/acscatal.0c03340
ACS Catal. 2020, 10, 13415−13436

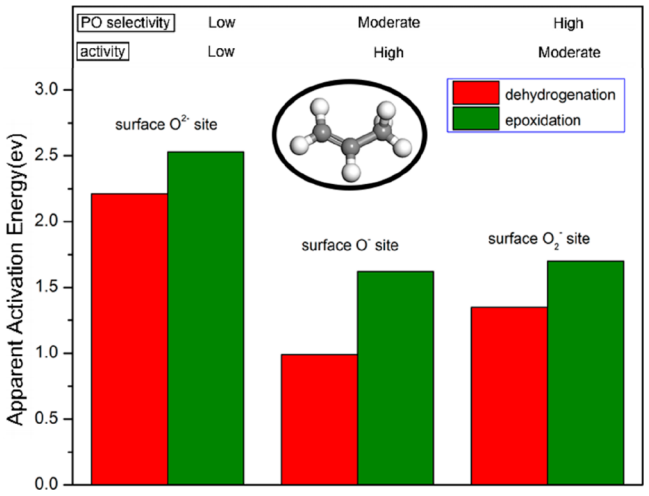

Figure 9. Analysis of the energetic span model with surface O^{2-}, O^{-}, and O_2^{-} species on $Cu_2O(111)$. Reproduced with permission from ref 45. Copyright 2018, American Chemical Society.

surface-bound O^{-}. For O^{-}, the activation barriers (ABs) for the transition states that lead to OMC formation are significantly higher than those for AHS (1.6 vs 1.0 eV, respectively), which results in acrolein being the predominant product. The most selective species is the surface-bound O_2^{-}. It is less reactive than O^{-} but more active than the lattice O^{2-}. For oxidation with O_2^{-}, the ABs for the transition states that lead to OMC formation are similar to those for AHS (1.65 vs 1.35 eV), which indicates that PO could form. With lattice O^{2-}, the AB for the ring-closing step that leads from OMC to the adsorbed propylene oxide is too high (2.2 eV) for any PO selectivity. However, in all cases the AB for the dehydrogenation route is lower, meaning that the catalyst requires modifications or doping to be selective for epoxidation.

Diekmann et al.[86] studied the effect of copper oxide particle size supported over SBA-15 on PO selectivity. According to their UV−vis analysis, increasing the Cu loading from 1.1 to 19.4 wt % increased the CuO cluster size from predominantly single-atom Cu^{2+} centers to nanometer-scale particles, presumably smaller than 3 nm. No crystalline CuO was detected in any of the catalysts. The cumulative selectivity of acrolein, CO, and CO_2 over all tested catalysts was above 90%. The PO selectivity was below 5% and exhibited a nearly linear positive correlation with the amount of bridging oxygen atoms ($Cu^{2+}-O^{2-}-Cu^{2+}$). The abundance of these species, identified and tentatively quantified by UV−vis−DR, increased with copper loading. Larger CuO particles give higher PO selectivity, whereas acrolein selectivity was independent of copper loading. The authors also allowed for the presence of a minor amount of Cu^{+} in the catalysts during the reaction, with the Cu^{+} fraction being higher in samples containing more copper.

Seubsai et al.[87] synthesized $Sb_2O_3-CuO-NaCl/SiO_2$ catalysts for selective propylene oxidation. The best-performing catalyst contained a Sb/Cu/Na ratio of 2/3/1 by weight and achieved a PO selectivity of 43% at 0.66% propylene conversion (Figure 10). The XRD analysis revealed that the coexistence of Sb_2O_3 and CuO crystalline phases is essential for PO formation and NaCl acts as a promoter by reducing further oxidation or isomerization of the products. Sodium chloride presumably occupies the most active sites on the catalyst surface and consequently decreases propylene conversion. A stability test showed a drop from the initial 0.95% C_3H_6 conversion to 0.65% at 10 h. The TGA-TPO and XRD analyses of spent catalysts identified sintering of CuO and Sb_2O_3, and not carbon accumulation, as the reason for deactivation.

Seubsai et al.[88] combined CuO with RuO_2 and modified it with NaCl, TeO_2, Cs_2O, and TiO_2. The best performance was achieved at a Ru/Cu ratio of 3 and after modification with NaCl; however, the catalyst deactivated rapidly. The deactivation was a result of the loss of Cl^{-} due to steam formed during the reaction. A recent report[89] indicates the occurrence of the oxochlorination reaction as the reason for chloride loss over silver catalysts. The best stability/activity/selectivity was measured when TeO_2 was used as the promoter. NH_3-TPD analysis revealed a decrease in strong acid sites when the latter promoter was added, which is the likely reason for increased PO selectivity. A PO selectivity of 47% at ∼0.35% C_3H_6 conversion was achieved, and the catalyst remained stable for 12 h.

Teržan et al.[73] investigated sub-nanometer CuO_x/SiO_2 catalysts containing 5 wt % Cu and modified with alkali (Na, K, Cs) and alkaline-earth (Ca) nitrate salts. *In situ* XANES revealed that, during the reaction, redispersion or flattening of

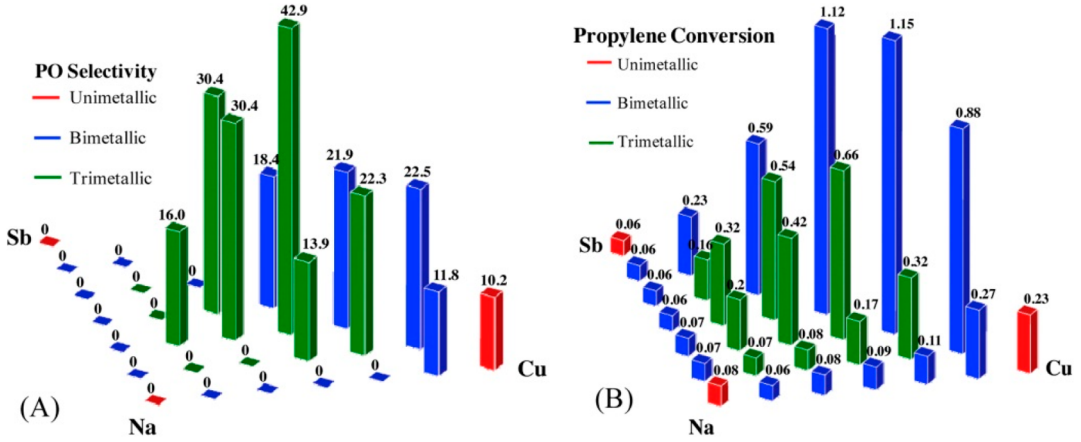

Figure 10. PO selectivities (A) and propylene conversion (B), both in percent, as a function of Sb−Cu−Na concentrations on the SiO_2 support at 250 °C. All catalysts had a total metal loading of 18 wt % and were calcined at 500 °C. Reproduced with permission from ref 87. Copyright 2015, Elsevier.

https://dx.doi.org/10.1021/acscatal.0c03340
ACS Catal. 2020, 10, 13415−13436

CuO_x clusters takes place and copper is predominantly in the Cu^+ oxidation state (25−70%); the rest is Cu^{2+} (Figure 11).

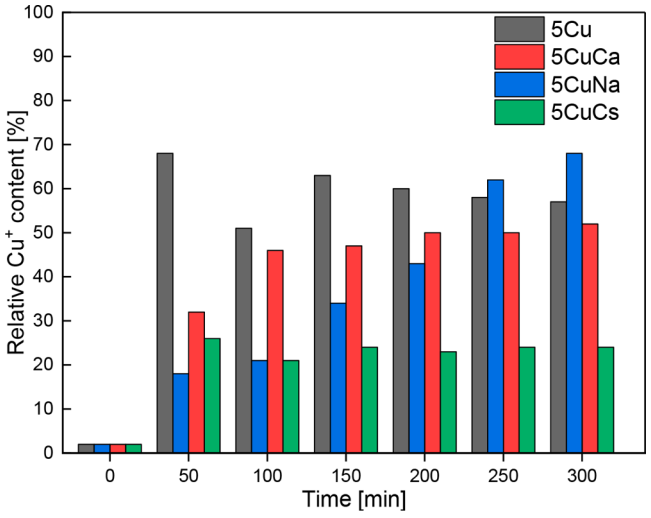

Figure 11. Evolution of the Cu^+ fraction as a function of TOS for the 5Cu, 5CuNa, 5CuCs, and 5CuCa catalysts. The uncertainty of the relative amountd of Cu^{2+} and Cu^+ is ±2%. Reproduced with permission from ref 90. Copyright 2020, Elsevier.

There was a minimal correlation between PO selectivity and fraction of Cu^+, showing that the presence of Cu^+ is not the sole determining factor governing PO selectivity. Also, no correlation was identified between the amount of Lewis acid sites and PO selectivity, most likely because of their weak strength on the KIT-6 silica morphology. The deactivation of catalysts due to CuO_x sintering was substantially decreased upon catalyst modification with both alkali and alkaline-earth metals. Cs acted as a most effective deactivation barrier, yielding no deactivation in 16 h of the reaction at 350 °C. Unmodified and Ca-modified catalysts did not produce any PO; they produced only acrolein and CO_x. The results of CO_2-TPD-DRIFTS showed that Na, K, and Cs modification (∼0.7 wt %) generated additional basic sites on the surface of the catalysts. These sites are likely electrophilic oxygen species, and if one considers that these are the only PO-selective catalysts, it appears that the most important factor in selective propylene epoxidation over CuO_x/SiO_2 catalysts is the electrophilic character of the oxygen species induced by the presence of Na, K, or Cs.

Teržan et al.[73] also tested the effect of cofeeding PO into the C_3H_6/O_2/He stream during the propylene oxidation reaction. The CuO_x/SiO_2 catalyst decomposed approximately 90% of cofed PO at 350 °C, whereas this fraction was slightly lower (75%) over Na-modified CuO_x/SiO_2. This confirms a very important contribution of PO oxidation upon readsorption on the catalyst surface and, even more importantly, via postcatalytic gas-phase radical reactions.

As a result, the selectivity of the catalyst that is being generally observed and reported is rather a combined catalytic/reactor contribution that needs to be untangled by shortening the residence time of reactants in order to boost PO selectivity.

To summarize, single-crystal studies identified CuO(111) as being more reactive for deep oxidation of propylene in comparison to Cu_2O(111).[79] Over the Cu_2O(111) surface, acrolein formation is favored, whereas the selectivity is shifted to CO_2 over Cu_2O(100).[77,78] A very good correlation with the single-crystal selectivity data provided above was obtained by Hua et al.[11] over unsupported nanoshaped Cu_2O particles. They confirmed the preferred selectivity of (111) and (100) facets for acrolein and CO_2 and additionally confirmed the (110) facet as being selective for PO. Upon dispersion of the CuO_x nanoparticles over different supports and alkali and/or halide modification, electronic and structural interactions strongly influence the PO selectivity. Consequently, the single-crystal results are crucial for understanding the structure, activity, and selectivity dependence of propylene epoxidation over Cu_2O, but the results are not necessarily transferable to predict the behavior of supported metal nanoparticles.

3.1. Theoretical DFT Analysis of Copper-Based Catalysts in Propylene Epoxidation. Kizilkaya et al. studied Ru−Cu(111) and Cu(111) surfaces.[51] The former was modeled as a monolayer (1 ML) of Cu(111) atoms over the Ru(0001) substrate, and the latter was used as a benchmark. On the Ru−Cu catalyst, propylene adsorbs more strongly (−0.38 vs −0.16 eV). However, this surface is much more active for AHS (E_A = 0.48 eV) than for OMMP1 formation (E_A = 0.92 eV), rendering it unsuitable for epoxidation. OMMP2 was not studied on the basis of thermodynamic grounds from previous studies. On Cu(111), however, the authors noted a reversed trend (E_a for OMMP = 0.75 eV; E_a for AHS = 0.83 eV). From OMMP1, PO forms on Cu(111) and would also form on Ru−Cu(111) with barriers of 1.28 and 1.12 eV, respectively, which are lower than the corresponding barriers for propanal formation (1.37 and 1.61 eV). Thus, while Ru−Cu(111) would improve the secondary chemistry (OMMP1 transformation to PO rather than propanal), it destroys the selectivity of the primary chemistry by facilitating the AHS reaction.

Instead of metallic copper, its oxides can also be used for epoxidation. Song and Wang with their co-workers studied CuO[91] and Cu_2O.[92] On CuO(111), adsorbed propylene will most probably undergo AHS (barrier of 0.26 eV) or form OMMP2 (0.25 eV), while OMMP1 formation (0.49 eV) is less favorable. From OMMP2, PO forms (barrier of 1.20 eV). On CuO(100), OMMP2 formation is also more likely (barrier of 0.31 eV) than AHS (0.36 eV). OMMP2 converts to PO with a barrier of 0.77 eV. In both cases, the conversion of OMMP1 or OMMP2 to propanal or acetone has a prohibitively high barrier, making PO and acrolein the only products. The energy barriers for the same chemical conversions are lower on the (100) facet. Microkinetic simulations showed that the turnover frequency for acrolein and PO production at identical reaction conditions is higher on the (100) facet in comparison to (111). The origin of this higher activity is attributed to the position of the 3d orbital of Cu atoms on the (100) facet, as calculated by PDOS. These are closer to the Fermi level in comparison to those of Cu sites on the (111) facet, making interaction with the approaching adsorbates easier and thus providing a better overlapping and hybridization of states. The formation of PO increases with temperature, while acrolein formation reaches a maximum of around 400 K for CuO(111) and 450 K for CuO(100). The selectivity for PO is much higher on CuO(100).

On Cu_2O, however, there is a starker difference between the (111) and (110) surfaces.[92] The (111) surface binds the adsorbates more strongly, but (110) is more suitable for PO production, while (111) produces mainly acrolein. On Cu_2O(111), OMMP1 and OMMP2 form more readily (1.22 and 0.90 eV) in comparison to acrolein (1.20, 1.16, and 0.12

https://dx.doi.org/10.1021/acscatal.0c03340
ACS Catal. 2020, 10, 13415−13436

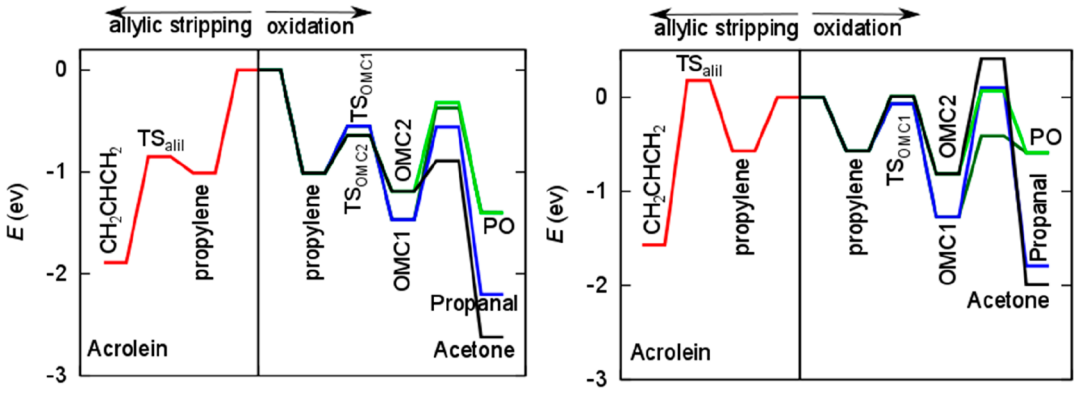

Figure 12. Potential energy surface of propylene oxidation on CuO (left) and Cs^+-modified CuO (right). Reproduced with permission from ref 90. Copyright 2020, Elsevier.

eV for the first AHS, O addition, and second AHS) but cannot undergo a rearrangement to yield PO due to excessively high barriers (1.92 and 1.59 eV). Instead, the AHS route is active. On $Cu_2O(110)$, however, OMMP2 predominantly forms (0.53 eV) and converts to PO (1.41 eV) and not acetone (1.60 eV). Although the AHS route is related to the basicity of oxygen, which is higher on the (110) surface, the prohibitively high second dehydrogenation barrier (1.89 eV) renders this route inactive.

Teržan et al.[90] used DFT to study the reaction on a bare $Cu_{12}O_{12}$ cluster and on the cluster with added Ca, Na, and Cs atoms (Figure 12). The propylene binding energy decreased from 1 eV to 0.4−0.6 eV upon doping, and the O_2 activation barrier decreased from 0.64 eV to 0.35−0.44 eV. Oxygen dissociation also became much more exothermic (from −0.79 eV to −2.24−2.62 eV) due to the high affinity of alkali and alkaline-earth metals toward oxygen.

The effect of Na^+ modification on selectivity is similar to that of Cs^+ but is more pronounced. The Na^+ modification decreases the activation barrier for the oxametallacycle (OMC) ring closure from 0.87 to 0.71 eV (in comparison to the pure copper oxide cluster). At the same time, the barrier for the abstraction of allylic hydrogen increased from 0.45 to 0.72 eV. This alkali modification negatively influenced the catalytic activity but notably improved the PO selectivity.

The opposite effect is achieved by Ca^{2+} addition: the activation barrier for OMC ring closure increased from 0.87 to 1.08 eV and that for allylic hydrogen stripping decreased from 0.45 to 0.16 eV. The group 2 metals (alkaline-earth metals) are not suitable dopants for CuO_x catalysts in propylene epoxidation. Direct insertion of atomic oxygen into the C=C bond of propylene (forming PO) was in all instances unlikely due to its high activation energy (0.92 eV for pure CuO and 1.44, 0.97, and 1.10 eV for the Na, Cs, and Ca modifications, respectively). A Bader charge analysis showed that the alkali and alkaline-earth doping acts very locally and an electronegativity change is localized only on the adjacent oxygen atoms sufficiently, to alter the reaction selectivity.

4. CHARACTERIZATION

Defining the exact mode of action of a catalyst and the associated promoter is a difficult task, often being overlooked or generalized by citing other publications with similar results. However, some guidelines can be established as a common thread throughout the publications to pave the way to improved catalysts. It is imperative that, in reporting WHSV values, these should be calculated per mass of the catalyst and take into account only the volume of the reactants, not the diluting gas. The feed composition, the reaction temperature (preferably measured in the middle of the catalyst layer), the conversion of reactants, and the selectivity toward the products should be reported in order to enable a more accurate comparison of catalytic performance and further calculation of productivity ($g/(g_{cat}\ h)$) or yields. Additionally, the temporal evolution of selectivity and activity (conversion) should be reported, since epoxidation catalysts are very sensitive to deactivation (sintering, oxidation, reduction, ...). Without detailed structural information on the active particles, in the case of very different activities of step vs terrace sites or in the case where the metal−support perimeter is the active site, calculations of TOF values are of limited informative value. Defining the former leads to an in-depth understanding of the mechanisms mentioned at the beginning of the chapter. Theoretical methods for electronic structure calculations (such as *ab initio* post-HF or DFT) can shed light on whether the increased yield is due to a geometric effect or an electronic effect. Is the increase a result of the change in the binding strength of the reactants, the products, or the intermediates? It is important to keep in mind that these calculations can only give trends and predictions, while the numerical values should be used with caution.

A widely available analytical technique is UV/vis spectroscopy. Such a basic technique can discern a great deal about the reaction mechanism as evidenced by Lu et al.,[32] who determined that Ag^+, formed by chlorine addition, is the site governing PO selectivity. This was also excellently implemented by Marimuthu et al.[74] in their photothermal epoxidation experiments. They used it to prove that the particles undergo light-induced reduction and that, while the catalysts are oxidized under only thermal conditions, they are successfully kept in a metallic state under photothermal conditions. Teržan et al.[73] also successfully used this technique under the reaction conditions to determine that sintering was the cause of catalyst deactivation. One will note that all of these experiments were performed *in situ*, which is a prerequisite, since catalysts are highly dynamic and change their structure and oxidation state as a function of atmosphere and temperature.

Chemisorption is also a very powerful and available technique. Lu et al.[32] used O_2 chemisorption to determine silver dispersion and used it to calculate the average particle size. Wang et al.[82] found, using temperature-programmed

https://dx.doi.org/10.1021/acscatal.0c03340
ACS Catal. 2020, 10, 13415−13436

desorption, that chlorine atoms on the surface may block active sites by forming an inert CuCl phase. Hua et al.[11] combined chemisorption with DRIFTS, which allowed them to conclude that Cu_2O epoxidation follows the MvK mechanism, as the lattice O atoms are the oxidizing species. The activity and selectivity of their catalyst were also correlated very well with their DRIFTS results and were additionally supported by DFT. Teržan et al.[73] combined CO_2 sorption with DRIFTS to probe the basicity of the active oxygen species, confirming a weakly nucleophilic character of surface oxygen, which is required for propylene epoxidation.

To determine the nanoparticle size and shape, grazing-incidence small-angle X-ray scattering (GISAXS) is a very powerful technique. Lei et al.[28] used it to determine the sintering of Ag_3 trimers, which allowed them to determine the temperature at which the catalytic reaction should be run. Very similar observations were noted by Cheng et al.[59]

Another very powerful tool to determine the particle size, shape, and terminating crystal plane is high-resolution transmission electron microscopy (HR-TEM). Hua et al.[11] used it to determine the different terminating planes of the Cu_2O nanocrystals and correlated this with the selectivity and activity of these nanocatalysts. Wang et al.[82] did the same for their Cu_2O nanocubes. Ghosh et al.[41] confirmed the terminating plane of their WO_3 support and the Ag nanoclusters, using *d* spacing measured by TEM. The same was achieved by Yu et al.,[14] for their Ag/La_2O_3 catalysts. Yang et al.[85] used scanning tunneling microscopy to confirm the formation of a $TiCuO_x$ mixed oxide. They combined these results with PO chemisorption and temperature-programmed desorption. In addition, they examined the adsorbed PO with high-resolution electron energy loss spectroscopy (HREELS) and X-ray photoelectron spectroscopy (XPS). With this, they were able to confirm the formation of the oxametallacycle upon PO adsorption, explaining the selectivity of the catalyst for PO.

Lei et al.[28] used XPS to prove that silver nanoparticles remain metallic during epoxidation, hinting at a L-H type mechanism. Hua et al.[11] confirmed the removal of the capping ligands from the Cu_2O nanocatalysts and minimal oxidation extent to CuO under the reaction conditions. Ghosh et al.,[41] with the help of XPS, confirmed the presence of Ag_2O under the reaction conditions. They claimed that the formation of this phase is essential for PO formation, which indicates a MvK type mechanism over Ag/WO_3 catalysts. Yu et al.[14] measured XPS and confirmed that molecular oxygen preferentially disassociates on the surface of La_2O_3 and migrates to the Ag−support interface. This implies that over Ag/La_2O_3 catalysts epoxidation follows a L-H type mechanism. Elucidating the reaction mechanism by fitting the steady-state kinetic data with rate expressions has been rarely practiced in the last few years.[34] Pu et al.[57] made a more elaborate comparison for ethylene epoxidation over silver catalysts and observed that "ethylene oxidation reaction kinetic studies have not been able to distinguish between L-H or E-R (L-R) reaction mechanisms and the different types of oxygen species present on Ag during ethylene oxidation, reflecting the inability of just kinetic studies to establish the fundamental molecular events." On the other hand, the MvK mechanism was proposed where participation of lattice oxygen was experimentally identified to participate in the oxidation reaction and was not based on an analysis of kinetic data.

Yu et al.[43] used XPS to confirm that there was indeed a lattice expansion seen in Ag, in the AgNi core−shell nanoparticles. They inferred that a geometric rather than an electronic effect is what alters the selectivity. The core−shell structure was additionally confirmed with the help of high-sensitivity low-energy ion scattering (HS-LEIS). Wang et al.[82] used HS-LEIS to investigate the amount of Cl^- in their catalysts, and confirmed that it is localized at the surface. Additionally, quasi *in situ* XPS was performed, which indicated that Cl^- depletion, and not the oxidation of Cu(I) to Cu(II), caused the drop in PO selectivity.

Synchrotron light is probably one of the most powerful tools in the investigation of nanoparticles. It allows for very sensitive XRD measurements, as evidenced by Yu et al.[43] With X-ray absorption spectroscopy (XAS), they additionally confirmed the size of their nanoparticles and showed the lattice expansion effect Ni had on Ag. Ghosh et al.[41] confirmed that in the fresh catalyst silver is indeed metallic, while during catalysis it oxidizes to Ag_2O. With this they confirmed an MvK-type mechanism over their catalysts. XAS also was proved to be a very useful technique for Teržan et al.,[73,90] since imaging of their particles with TEM proved to be impossible. With the help of XAS they calculated the size of their particles, confirmed the mode of action of the promoters, and additionally confirmed an MvK-type mechanism for their catalysts. Synchrotron irradiation can also drastically increase the sensitivity of XPS, especially if it is performed at higher pressures, as evidenced by Lei et al.[28] and Hua et al.[11]

Note that most of the techniques reported in this chapter were performed *in situ*. For accurate and representative measurements, *in situ* and if possible even *operando* measurements are crucial. These would enable a direct correlation of changes in the material with changes in selectivity, activity, or both.

5. DISCUSSION AND CONCLUSIONS

This chapter contains a discussion and conclusions that can be made, on the basis of the reviewed literature, and proved efficient for improving PO selectivity.

5.1. Silver-Based Catalysts. *5.1.1. Alkali and Halide Modification.* Modification of silver surfaces with alkali cations consistently increases PO selectivity, with Na generally being the most efficient. This is a consequence of increasing both AHS and OMC activation barriers, where the former increases more.

Halides, especially chloride, have a positive effect on PO selectivity, but this time through increasing the AHS activation barrier and decreasing the desorption energy of OMC as PO. However, a catalytic activity decrease of about 1 order of magnitude is commonly observed by the presence of both alkali and halide in comparison to pure Ag. As a result, their content should be fine-tuned to maximize the PO weight time yield.

5.1.2. Support Effect. Although all chemistry essentially stems from the interplay of electronic density (primarily of valence electrons), the effect of heterogeneous catalysts is usually decomposed into an electronic or geometric effect. An electronic effect pertains to the change in electronic density (such as the famous d band model descriptor[93]), while the geometric effect is caused by imposed geometry limitations. Often, a third synergetic effect is also at play.[94] In calculations, these effects can be separately captured by the interaction and distortion energies.[95] Catalyst supports influence the reactions

https://dx.doi.org/10.1021/acscatal.0c03340
ACS Catal. 2020, 10, 13415−13436

through both mechanisms: they can change the electron density of the active material, and they can force it to assume structures, which are more conducive to higher selectivities.

A considerable positive support effect on PO selectivity was observed when silver was dispersed over La_2O_3,[14] WO_3,[41] MoO_3,[31] and Y_2O_3,[30] in comparison to Al_2O_3 or SiO_2. This effect cannot be explained simply in terms of Lewis acidity because La_2O_3 and Y_2O_3 are less acidic than Al_2O_3, while WO_3 and MoO_3 are more acidic, yet all of them outperform Al_2O_3 (Figure 13). By definition, acidic supports are efficient electron

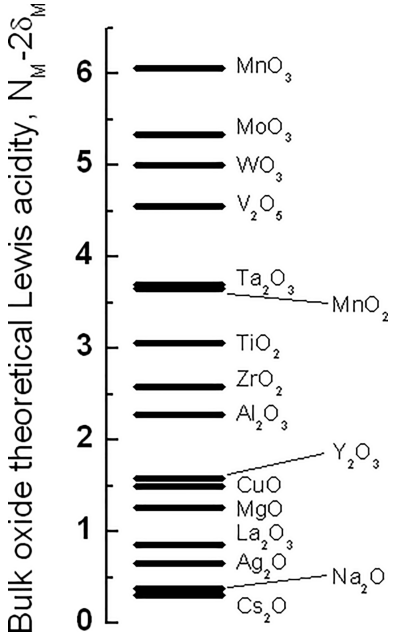

Figure 13. Theoretical bulk oxide Lewis acidity of different metal oxides determined as $N_M - 2\delta_M$, where N_M represents the formal oxidation state and δ_M is Sanderson's partial charge of the cations in the bulk oxides.[98] The figure was redrawn with data published by Jeong et al.[98]

donors, whereas basic oxides are electron acceptors, which is mirrored in a different fashion of oxygen activation. Lewis bases, such as La_2O_3, facilitate the dissociation of molecular oxygen. Additionally, it is the atomic structure of the supported Ag active clusters, in turn influenced by the support, which governs the PO selectivity. Supports favoring the formation of the Ag(100) facets positively affect the selectivity because of the higher selectivity of that facet. The WO_3 support, being a strong Lewis acid, does not increase oxygen dissociation but enhances the reaction by elongating the Ag−O bond in Ag_2O, facilitating oxygen addition to the propylene C=C bond.

Supports also affect the product formed. They can facilitate PO isomerization, which leads to total combustion. This effect has been noticed and examined by several researchers.[73,84,96,97] The common thread is that acidic supports, even if they exhibit moderate Lewis acidity such as amorphous silica,[18,73,86,98] should be avoided. If an acidic support is used, it should be modified, where the acid sites are neutralized by titrating with a basic promoter.

5.1.3. Silver Particle Shape. The atomic arrangement on continuous Ag crystalline planes results in a different strength of Ag−O binding.[12] The surfaces with a stronger Ag−O binding have a lower activation barrier for OMC formation, giving a higher probability for the oxidation selectivity to shift toward epoxidation. This makes Ag(100) more selective toward PO than Ag(111). Furthermore, the Ag−Ag distances can be modified by employing a suitable synthesis technique that produces Ag nanoshapes that exhibit preferentially Ag(100)-terminated crystalline planes or through the growth of thin Ag layers in an epitaxial manner, where the packing arrangement and size of the support atoms will determine the extent of Ag−Ag bond elongation.[43] As a result, facile synthesis methods being able to produce (nano)cube shaped Ag nanoparticles exposing predominantly (100) crystalline planes or metal core−Ag shell particles appear as viable starting points for more selective propylene epoxidation catalysts.

5.1.4. Silver Particle Size. There is a strong particle size effect influencing the PO selectivity, which governs the fraction and reactivity of oxygen species at the support, Ag−O interface, and terminating Ag crystalline planes. However, the interface appears to have a very contradictory effect, which depends on the nature of the support: Al_2O_3[28] vs La_2O_3.[14] Over small Ag clusters on α-Al_2O_3, the highly active oxygen species located at the Ag−support interface are dominant and prefer allylic hydrogen stripping. Such active sites preferentially produce acrolein and favor total propylene oxidation.[28,59] However, contradictory evidence exists:[99] namely, that water can easily dissociate on coordinatively unsaturated surface Al sites to form a hydroxylated Al_2O_3 surface. The activation of molecular oxygen via a hydroperoxyl (OOH) intermediate (i.e., O_2 abstracting a hydrogen atom from vicinal H/OH sites) was identified as a feasible pathway. Water produced via the total propylene oxidation reaction dissociates to H/OH pairs which enable the H-transfer process by constructing a hydrogen-bonding chain with adsorbed O_2. The resulting OOH turns out to be a key oxidative species for subsequent propylene epoxidation. Over reducible oxides which favor catalytic turnovers via the Mars−van Krevelen mechanism, the adsorbed-water-mediated O_2 activation mechanism coexists with that of oxygen activation over oxygen vacancies.[100]

The optimal silver particle size, giving the highest PO selectivity, is reported to be in the range between 20 and 40 nm. However, the metal−support interaction is constrained to the interface parameter extending 1 nm at best,[101] suggesting that either the actual active sites were overlooked or they are the terrace sites of the exposed Ag facets. This calls for more thorough and systematic approaches toward the identification of structure−selectivity relationships, where it has to be ensured that the catalytic and postcatalytic effects (*vide infra*) are clearly untangled.

5.1.5. Reaction Conditions. In addition to catalyst design and chemical composition, reaction conditions such as temperature, total pressure, and partial pressure of oxygen and propylene appear to be equally important for PO selectivity.

The partial pressure of oxygen strongly increases propylene conversion but simultaneously decreases PO selectivity.[16,25,26] The same trend in catalytic performance is generally observed also with reaction temperature. Carbonio et al.[102] demonstrated, using transient *in situ* XPS analysis, that diatomic oxygen is present at very low O coverages (<0.04 ML) on a Ag(110) surface, at low temperature. The dissociation of diatomic oxygen species to monatomic species is always thermodynamically favored under epoxidation conditions.[103] The presence of diatomic oxygen species on the surface under equilibrium conditions is unlikely. However, at low oxygen pressures and consequently low oxygen surface coverages,

https://dx.doi.org/10.1021/acscatal.0c03340
ACS Catal. 2020, 10, 13415−13436

surface diatomic oxygen species could exist[104,105] if their dissociation was kinetically limited, as suggested by microkinetic modeling.[102,106] These oxygen species are electrophilic and are considered selective for epoxidation; thus, the reaction conditions should be adjusted to maximize their presence. The use of oxygen-permeable membrane reactors and the use of a staged oxygen feed appear to be beneficial strategies for improving PO selectivity while keeping the oxygen concentration in the reactor low.

5.1.6. Elevated Pressure. The effect of total reaction pressure (experimentation at elevated pressure) has rarely been investigated, and the vast majority of published work has been performed at ambient or slightly elevated pressure (below 1.5 bar). However, encouraging results of both PO selectivity as well as catalytic activity have been reported over Ag/WO_3 in the pressure range between 2 and 30 bar,[41] suggesting the generally investigated atmospheric pressure conditions are the easiest to achieve but are not optimal. Theoretical calculations suggest that the surface coverage with olefins increases more quickly at elevated pressures, resulting in higher activity and selectivity.[19] Also, the industrial propylene epoxidation reaction with molecular oxygen will inevitably run at elevated pressure due to the economics of downstream processes, mostly separation via distillation. As a result, more studies at elevated pressures are required.

5.2. Copper-Based Catalysts. *5.2.1. Reaction Mechanism.* In contrast to silver-based catalysts, which are metallic during propylene epoxidation, a prevailing consensus is that Cu^+ is the predominant oxidation state over copper-based catalysts. Namely, a substantial fraction of Cu^{2+} is reduced to Cu^+ (in starting from the oxidized catalyst) or is oxidized from Cu^0 to a mixture of Cu^{2+} and Cu^+ (when the catalyst is reduced prior to catalysis[83]). In addition, the presence of different adsorbed oxygen species (O_2^-, O^-, and O^{2-}) originating from molecular oxygen activation allows for a parallel occurrence of epoxidation reactions via lattice or adsorbed oxygen species. These pathways are entangled and are not trivial to separate in real catalytic systems.

5.2.2. Oxygen Species. DFT analyses over the Cu_2O (111) surface[45] show that activation barriers for OMC formation and ring closure depend strongly on the oxygen species involved: O_2^- is the most selective for PO formation, O^- is the most reactive and favors acrolein formation via AHS, whereas O^{2-} has a high activation barrier for OMC ring closure, meaning it is not selective for PO.

This can be extended also to other copper oxidation states (Cu^0 and Cu^{2+}), meaning that further studies should focus on chemical compositions and copper surface geometries that stabilize these electrophilic oxygen species.

The adsorbed electrophilic diatomic oxygen species are more selective toward PO, and it is thus desirable for the L-H mechanism to dominate the reaction.

5.2.3. CuO_x Particle Shape. The terminating Cu_2O crystalline planes also have a pronounced effect on the binding geometry of oxygen and consequently for PO selectivity. By steering the Cu_2O crystallite shape into (nano)cubes, consequently favoring the (100) crystalline plane over the thermodynamically most stable (111), PO selectivity can be boosted.

5.2.4. CuO_x Particle Size. There is a strong selectivity dependence on the CuO_x particle size, where smaller particles are more selective toward PO, whereas larger particles favor acrolein. The origin of this structure selectivity likely lies in the relatively higher fraction of coordinatively unsaturated step and kink oxygen sites in the small CuO_x nanoclusters in comparison to large CuO_x crystals. The *lattice* oxygen in the small CuO_x nanoclusters has a lesser nucleophilic character and is thus more selective. The propylene epoxidation reaction is generally run between 250 and 350 °C. This temperature surpasses the Hüttig temperature (T_H) of Cu, Cu_2O, and CuO. The T_H value indicates the onset of notable mobility of surface copper atoms, and these values are ∼135, 180, and 207 °C for Cu, Cu_2O, and CuO, respectively. As a result, at typical propylene epoxidation temperatures, a notable mobility of surface copper atoms can be expected, which will ultimately result in sintering and loss of the most selective CuO_x morphology. Sintering of silver trimers supported over amorphous alumina films was observed during propylene oxidation starting at about 110 °C,[28] which is remarkably close to the calculated Hüttig temperature of silver, which is 100 °C.

5.2.5. Alkali Modification. The alkali modification of copper-based catalysts generally improves PO selectivity but also simultaneously decreases catalytic activity. The modification by alkali cations has a very short range: i.e., it is localized only at adjacent oxide anions. Considering that the optimum PO yield is generally achieved at an alkali/copper molar ratio of ∼0.05−0.1, a notable fraction of CuO_x oxide anions still remains unaffected, which limits the maximum achievable PO selectivity. As a result, despite proven effectivity over both silver and copper catalysts, alkali modification alone is unlikely to enable the PO productivity desired by industrial standards.

5.2.6. Chemical Engineering Approach. The majority of propylene epoxidation research is focused entirely on catalyst design to improve PO selectivity, while the aspect of reactor engineering remains largely overlooked. The use of high reaction temperatures ensures appreciable propylene conversion, but the PO formed is vulnerable to total oxidation upon readsorption on the catalyst surface or in the postcatalytic (heated) part of the reactor due to thermal, noncatalytic reactions (Figure 14).[107,108] The residence time in

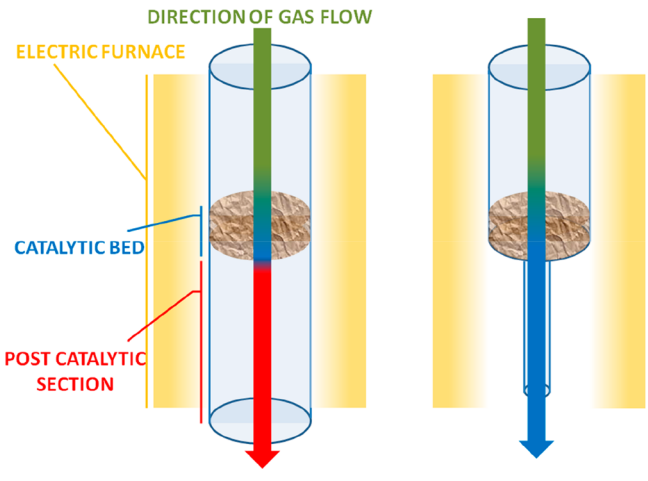

Figure 14. Schematic representation of a conventional, externally heated fixed bed tubular reactor (left-hand side). The downward arrow shows the gas flow direction with blue emphasizing the section of the reactor where catalytic reactions occur and red representing the section of dominant noncatalytic reactions. By a decrease in the the postcatalytic reactor volume (and thus the residence time), the contribution of noncatalytic reactions can be minimized (right-hand side).

https://dx.doi.org/10.1021/acscatal.0c03340
ACS Catal. 2020, 10, 13415−13436

the postcatalytic section of a typical laboratory-scale tubular fixed bed reactor is often about 1 order of magnitude longer in comparison to the residence time in the catalytic bed. Also, the temperature in the postcatalytic part of the reactor is usually very similar to those in the catalytic bed. This gives PO sufficient time to convert further to CO_x and H_2O. To overcome this downside, the reactor should be engineered to minimize the volume of the heated, postcatalytic volume as much as possible and thus shorten the exposure of PO to high temperatures. Alternatively, the use of nonconventional microwave heating of the catalyst localizes heat only at the catalytic bed, but the catalyst has to be able to absorb the microwaves.

In the following paragraphs, we identify the most efficient method of catalyst modification. Since the propylene oxidation experiments in the analyzed literature were performed under broadly different conditions, such as reaction temperature, catalyst mass, total flow rates, gas concentrations, reactor types, and total pressure, a direct comparison of rates, conversions or selectivities is not sensible. As a result, we adopted the approach proposed by van Deelen et al.[101] The PO yield of modified catalysts was compared to a (nonmodified) reference catalyst reported in the same paper. Thus, both catalysts were investigated and compared under the same conditions. Consequently, a PO productivity enhancement factor for the modified catalyst over the reference calculated was calculated (Figure 15A). The PO productivity enhancement factor was calculated as $\frac{\text{PO yield}_{\text{modified catalyst}}}{\text{PO yield}_{\text{nonmodified catalyst}}}$, as this parameter takes into account all contributions from activity and selectivity.

Catalyst selectivity modification by alkali and halide doping is by far the most often researched, and PO productivity enhancements up to 40 can be obtained (Figure 15A). However, in most cases, the PO yield increases up to 10-fold. The strategy of tailoring size or shape of nanoparticles, thus exposing certain facets, or modifying interatomic distances appears to be the least successful, as up to 7-fold enhancements are reported. The support effect is moderate, except for the 31.7-fold PO productivity gain shown for Ag nanocubes on La_2O_3 in comparison to Ag nanocubes on Al_2O_3.[14]

The most successful engineering approach appears to be running the reaction at 20 bar and using a membrane reactor, which enabled up to a 30-fold PO productivity gain. Also, silver-based catalysts appear to be more prone to improvement by the reviewed strategies; however, this might also be due to substantially more research done on silver in comparison to copper.

Figure 15B shows PO selectivity as a function of Ag or CuO_x particle size. For Ag-based catalysts, it appears that an active metal cluster measuring about 5 nm enables the highest PO selectivity, which drops strongly as the Ag particle size decreases. This suggests the negative effect of steps and kinks or of metal−support Ag sites on PO selectivity, as these coordinatively unsaturated sites are generally more abundant in smaller nanoparticles.[110] For copper-based catalysts, there are much fewer experimental data available and the optimal Cu_2O cluster size still remains to be identified. However, there appears to be a positive correlation between the Cu_2O size and PO selectivity. One also has to bear in mind that data shown in Figure 15B include both bulk and supported nanoparticles and the support effect on PO selectivity can be huge. As a result, the trends extracted have to be used with caution, until a larger

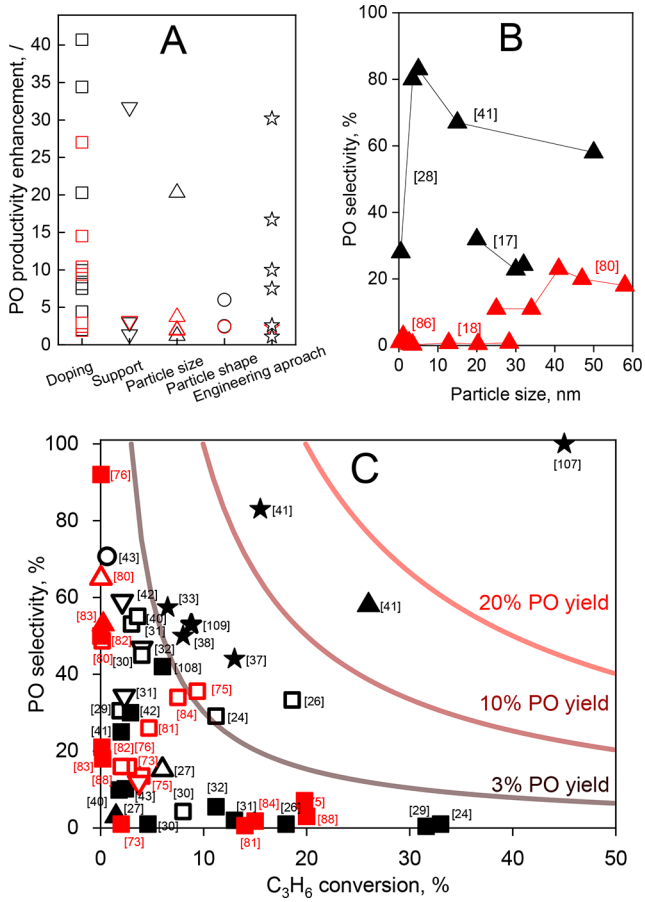

Figure 15. (A) PO productivity enhancement achieved over silver (black symbols)- and copper-based catalysts (red symbols) using different strategies: doping by alkalis, halides, or both[16,19,20,22−24,61,63,66,74,82−86] (squares), support effects[14,31,42,75] (downward triangles), particle size effects,[28,41,80,83,86] (upward triangles), particle shapes[11,14,43] (circles), and engineering approach[33,34,37,41,74,107−109] (stars). (B) PO selectivity as a function of particle size for copper (red triangles)- and silver-based catalysts (black triangles). (C) PO selectivity vs propylene conversion plot for various copper (red)- and silver-based catalysts (black) before (full symbols) and after modification (empty symbols).

body of data are accessible that would show a more reliable size−selectivity dependence.

Figure 15C compares the PO selectivity as a function of propylene conversion for Ag- and CuO_x-based catalysts. The majority of nonmodified catalysts (full symbols) lie very close to the *X* axis, revealing their poor PO selectivity despite notable activity. On the other extreme, there are several copper-based catalysts (full red symbols) which lie on the *Y* axis and exhibit above 20% PO selectivity, but at propylene conversions well below 1%. PO yields above 3% are interestingly silver-based catalysts from early patent literature[37,38,108] or reactions performed in a membrane reactor.[33] The 3% PO yield was exceeded only after catalyst modification: namely, catalyst doping with NaCl[24,26] or NaCl-promoted $CuO−RuO_2/SiO_2$.[75] On the basis of these data, catalyst modification with NaCl appears to be the most efficient for increasing the PO yield.

Exceptional results were reported over Ag/WO_3 nanorod catalysts with PO yields of about 15%, obtained at 20 bar reaction pressure.[41] The same authors were able to improve

https://dx.doi.org/10.1021/acscatal.0c03340
ACS Catal. 2020, 10, 13415−13436

the performance of their 5 wt % Ag/WO_3 nanorod catalyst to 45% PO yield when the reaction was operated at 30 bar and 375 °C.[109]

In addition to activity and PO selectivity, PO productivities in excess of 1 g PO/(g_{cat} h) are required for industrial application. Klemm et al. report 1 g PO/(g_{cat} h) as a threshold value for direct propylene epoxidation with O_2 to be competitive with existing PO producing technologies.[111,112] Table 5 compares the PO productivities over various catalysts and under different reaction conditions.

Table 5. Comparison of PO Productivity for Different Silver- and Copper-Based Catalysts

catalyst	temp, °C	PO productivity, g/(g_{cat} h)	ref
Ag (5 wt % NaCl)	350	0.295	24
Ag (3.8 wt % NaCl)	350	0.055	26
45 wt % $Ag/CaCO_3$ (1.7 wt % K_2CO_3)	210	0.025	27
Ag (50 mol % CuCl)	350	0.18	29
20 wt % Ag/α-Al_2O_3 (0.1 wt % Y_2O_3 and 0.1 wt % K_2O)	245	0.17	30
50 wt % Ag/MoO_3	400	0.025	31
56 wt % $Ag/CaCO_3$ (1 wt % NaCl)	260	0.01	32
Ag−Sr_2O_3/α-Al_2O_3[a]	240	1.74	33
3 wt % Ag-0.15 wt % $Cu/BaCO_3$	200	0.04	40
4.8 wt % Ag/WO_3 nanorods[b]	250	3.54	41
20 wt % Ag-3.75 wt % Mo-1.25 wt % W/ZrO_2	460	0.012	42
5 wt % Ag cubes/La_2O_3	270	0.056	14
5 wt % Cu/SiO_2 (0.8 wt % KNO_3)	350	0.084	73
2 wt % Cu-5 wt % Ru/SiO_2 (1.75 wt % NaCl)	300	0.57	75
1 wt % Cu/SBA (K/Cu = 0.7)	350	0.31	81
5 wt % Cu/SiO_2	225	0.005	83
3.6 wt % CuO-10.7 wt % RuO_2-0.25 wt % TeO_2/SiO_2	250	0.25	88
5 wt % Ag/microporous glass membrane (0.25 wt % Cs)	250	0.038	34
40% $Ag/CaCO_3$ (2 wt % K, 4.7 wt % W)[a]	258	0.0067	37

[a]Membrane reactor. [b]Operated at 20 bar.

Among the data reviewed, only Ghosh et al.[41] and Bere et al.[33] surpass the threshold value and report productivity of 3.5 and 1.7 g PO/(g_{cat} h) under optimal reaction conditions. All others fall 1−2 orders of magnitude short. As a result, active catalysts are still required with proven long-term stability, which can yield PO at an industrially relevant productivity.

6. FUTURE PROSPECTS

On the basis of the data collated above, the following directions for better silver- and copper-based propylene epoxidation catalysts can be outlined.

The development of new synthesis techniques for shaped Cu_2O and Ag nanoparticles is required, thus maximizing the exposure of the most selective facets and ensuring a high density of active sites though a sufficient specific surface area of the synthesized powders.

To better understand the role of different oxygen species on selectivity over CuO_x catalysts, further research should be focused on unraveling the reaction mechanism through studies using isotopic oxygen ($^{18}O_2$) to provide quantitative evidence of the contribution of lattice oxygen and adsorbed oxygen species derived from gaseous O_2 in the formation of acrolein, PO, CO_x, and other C3 oxygenates.

In situ and *operando* analyses are very often the only means of capturing the true working state of the catalyst and identifying the active sites. DFT analyses forecast that diatomic oxygen species are more selective regardless of copper oxidation state (Cu, Cu_2O, or CuO), meaning that further experimental studies should focus on chemical compositions and surface geometries that stabilize these electrophilic oxygen species, while the reaction is monitored by *in situ* DRIFTS, Raman,[12] or NAP-XPS techniques.[102]

Computational chemistry has, in recent years, increased our ability to analyze the catalytic reactions in detail, unavailable by experimental techniques. The methods are getting more precise and models increasingly complex to capture the intricacies of the experiment. All this is ushering in a shift from using electronic state calculations (mostly DFT) to explain the reaction mechanism on chosen surfaces to performing systematic screening. Using correlations and scaling relations, it is possible to extend the calculation of the reaction potential energy surface from a handful of surfaces to the whole periodic table, which might reveal better and "unexpected" epoxidation catalysts. Machine learning is a nascent technology with the possibility of delivering a large amount of data, making "periodic table"-wise screening campaigns seamless.

On the basis of the catalyst performance evaluation in Figure 15, it appears that a combination of strategies (Figure 15A) will be required to reach a breakthrough in propylene epoxidation with oxygen. We would like to see more interdisciplinary research being done, encompassing catalysis, chemistry (*in situ* and *operando* spectroscopy), and chemical engineering. In such an approach, a promising catalyst formulation (based on the currently available literature data) would be deposited and tested in a convection flow membrane reactor. A membrane reactor is preferred to shorten the residence time in the catalytic layer and minimize PO deep oxidation upon readsorption on the catalyst. In this way, catalytic and noncatalytic (thermal) contributions could be untangled. A range of reaction pressures can be tested, which, according to Ghosh et al.,[41] could lead to a significant increase in PO selectivity and productivity. The effect of reaction pressure has currently not been investigated in the convective flow membrane reactor in the propylene epoxidation reaction. To observe the phenomena occurring on the catalyst surface, the reactor could be upgraded to allow for *in situ* probing with relevant techniques, such as Raman, UV−vis, IR, XRD, and XAS, to analyze the working state and surface species involved in the catalytic epoxidation.

AUTHOR INFORMATION

Corresponding Author

Petar Djinović − *National Institute of Chemistry, SI-1001 Ljubljana, Slovenia; University of Nova Gorica, 5000 Nova Gorica, Slovenia;* orcid.org/0000-0002-5974-9118; Email: petar.djinovic@ki.si

Authors

Janvit Teržan − *National Institute of Chemistry, SI-1001 Ljubljana, Slovenia; Jožef Stefan International Postgraduate School, SI-1000 Ljubljana, Slovenia;* orcid.org/0000-0001-5528-5355

https://dx.doi.org/10.1021/acscatal.0c03340
ACS Catal. 2020, 10, 13415−13436

Matej Huš − *National Institute of Chemistry, SI-1001 Ljubljana, Slovenia;* orcid.org/0000-0002-8318-5121
Blaž Likozar − *National Institute of Chemistry, SI-1001 Ljubljana, Slovenia;* orcid.org/0000-0001-9194-6595

Complete contact information is available at: https://pubs.acs.org/10.1021/acscatal.0c03340

Notes

The authors declare no competing financial interest.

■ ACKNOWLEDGMENTS

J.T., M.H., B.L., and P.D. appreciate the funding by the Slovenian Research Agency (ARRS) under Core Grants P2-0152 and P2-0150.

■ REFERENCES

(1) Arntz, D.; Höpp, M.; Jacobi, S.; Sauer, J.; Ohara, T.; Sato, T.; Shimizu, N.; Prescher, G.; Schwind, H.; Weiberg, O. Acrolein and Methacrolein. In *Ullmann's Encyclopedia of Industrial Chemistry*; Wiley-VCH: Weinheim, Germany, 2000. DOI: 10.1002/14356007.a01_149.
(2) Papa, A. J. Propanal. In *Ullmann's Encyclopedia of Industrial Chemistry*; Wiley-VCH: Weinheim, Germany, 2011. DOI: 10.1002/14356007.a22_157.pub2.
(3) Papa, A. J. Propanols. In *Ullmann's Encyclopedia of Industrial Chemistry*; Wiley-VCH: Weinheim, Germany, 2000. DOI: 10.1002/14356007.a22_173.
(4) Sifniades, S.; Levy, A. B. Acetone. In *Ullmann's Encyclopedia of Industrial Chemistry*; Wiley-VCH: Weinheim, Germany, 2000. DOI: 10.1002/14356007.a01_079.
(5) BCC Research LLC. *CHM102A Olefin Derivatives: Global Markets to 2022*; 2018.
(6) Sienel, G.; Rieth, R.; Rowbottom, K. T. Epoxides. In *Ullmann's Encyclopedia of Industrial Chemistry*; Wiley-VCH: Weinheim, Germany, 2000. DOI: 10.1002/14356007.a09_531.
(7) Nexant Inc. *Market Analytics: Propylene Oxide - 2018*; 2018.
(8) Khatib, S. J.; Oyama, S. T. Direct Oxidation of Propylene to Propylene Oxide with Molecular Oxygen: A Review. *Catal. Rev.: Sci. Eng.* **2015**, *57* (3), 306−344.
(9) Lin, M.; Xia, C.; Zhu, B.; Li, H.; Shu, X. Green and Efficient Epoxidation of Propylene with Hydrogen Peroxide (HPPO Process) Catalyzed by Hollow TS-1 Zeolite: A 1.0 Kt/a Pilot-Scale Study. *Chem. Eng. J.* **2016**, *295*, 370−375.
(10) Blanckenberg, A.; Malgas-Enus, R. Olefin Epoxidation with Metal-Based Nanocatalysts. *Catal. Rev.: Sci. Eng.* **2019**, *61* (1), 27−83.
(11) Hua, Q.; Cao, T.; Gu, X.-K.; Lu, J.; Jiang, Z.; Pan, X.; Luo, L.; Li, W.-X.; Huang, W. Crystal-Plane-Controlled Selectivity of Cu_2O Catalysts in Propylene Oxidation with Molecular Oxygen. *Angew. Chem., Int. Ed.* **2014**, *53* (19), 4856−4861.
(12) Pulido, A.; Concepción, P.; Boronat, M.; Corma, A. Aerobic Epoxidation of Propene over Silver (111) and (100) Facet Catalysts. *J. Catal.* **2012**, *292*, 138−147.
(13) Ranney, J. T.; Bare, S. R.; Gland, J. L. The Role of Water in Propylene Partial Oxidation: Thermal Desorption Studies on Ag(110). *Catal. Lett.* **1997**, *48* (1−2), 25−29.
(14) Yu, B.; Ayvalı, T.; Wang, Z.-Q.; Gong, X.-Q.; Bagabas, A. A.; Tsang, S. C. E. Gas Phase Selective Propylene Epoxidation over La_2O_3-Supported Cubic Silver Nanoparticles. *Catal. Sci. Technol.* **2019**, *9* (13), 3435−3444.
(15) Christopher, P.; Linic, S. Shape- and Size-Specific Chemistry of Ag Nanostructures in Catalytic Ethylene Epoxidation. *ChemCatChem* **2010**, *2* (1), 78−83.
(16) Henriques, C.; Portela, M. F.; Mazzocchia, C.; Guglielminotti, E. A Comparison Between Epoxidation and Degradation of Ethylene and Propylene over Silver. *Studies Surf. Sci. Catal.* **1993**, 1995−1998.
(17) Zhang, Q.; Guo, Y.; Zhan, W.; Guo, Y.; Wang, L.; Wang, Y.; Lu, G. Gas-Phase Epoxidation of Propylene by Molecular Oxygen over $Ag/BaCO_3$ Catalysts: Effect of Preparation Conditions. *Catal. Today* **2016**, *276*, 2−10.
(18) Guo, L.-L.; Yu, J.; Wang, W.-W.; Liu, J.-X.; Guo, H.-C.; Ma, C.; Jia, C.-J.; Chen, J.-X.; Si, R. Small-Sized Cuprous Oxide Species on Silica Boost Acrolein Formation via Selective Oxidation of Propylene. *Chin. J. Catal.* **2021**, *42* (2), 310−319.
(19) Huš, M.; Hellman, A. Ethylene Epoxidation on Ag(100), Ag(110), and Ag(111): A Joint Ab Initio and Kinetic Monte Carlo Study and Comparison with Experiments. *ACS Catal.* **2019**, *9* (2), 1183−1196.
(20) Bielanski, A.; Haber, J. *Oxygen in Catalysis*; CRC Press: 1990; Vol. *29*.
(21) Huš, M.; Hellman, A. Dipole Effect on Ethylene Epoxidation: Influence of Alkali Metals and Chlorine. *J. Catal.* **2018**, *363*, 18−25.
(22) Akimoto, M. Kinetic and Adsorption Studies on Vapor-Phase Catalytic Oxidation of Olefins over Silver. *J. Catal.* **1982**, *76* (2), 333−344.
(23) Carley, A. F.; Davies, P. R.; Roberts, M. W. Oxygen Transient States in Catalytic Oxidation at Metal Surfaces. *Catal. Today* **2011**, *169* (1), 118−124.
(24) Lu, J.; Luo, M.; Lei, H.; Li, C. Epoxidation of Propylene on NaCl-Modified Silver Catalysts with Air as the Oxidant. *Appl. Catal., A* **2002**, *237* (1−2), 11−19.
(25) Farinha Portela, M.; Henriques, C.; Pires, M. J.; Ferreira, L.; Baerns, M. Catalytic Epoxidation and Degradation of Propylene by Dioxygen over Silver. *Catal. Today* **1987**, *1* (1−2), 101−110.
(26) Lu, G.; Zuo, X. Epoxidation of Propylene by Air over Modified Silver Catalyst. *Catal. Lett.* **1999**, *58* (1), 67−70.
(27) Zemichael; Fessehaye, W.; Palermo, A.; Tikhov, M. S.; Lambert, R. M. Propene Epoxidation over K-Promoted $Ag/CaCO_3$ Catalysts: The Effect of Metal Particle Size. *Catal. Lett.* **2002**, *80* (3/4), 93−98.
(28) Lei, Y.; Mehmood, F.; Lee, S.; Greeley, J.; Lee, B.; Seifert, S.; Winans, R. E.; Elam, J. W.; Meyer, R. J.; Redfern, P. C.; Teschner, D.; Schlögl, R.; Pellin, M. J.; Curtiss, L. A.; Vajda, S. Increased Silver Activity for Direct Propylene Epoxidation via Subnanometer Size Effects. *Science (Washington, DC, U. S.)* **2010**, *328* (5975), 224−228.
(29) Luo, M.; Lu, J.; Can, L. Epoxidation of Propylene over Ag-CuCl Catalysts Using Air as the Oxidant. *Catal. Lett.* **2003**, *86* (1/3), 43−49.
(30) Yao, W.; Lu, G.; Guo, Y.; Guo, Y.; Wang, Y.; Zhang, Z. Promotional Effect of Y_2O_3 on the Performance of Ag/α-Al_2O_3 Catalyst for Epoxidation of Propylene with Molecular Oxygen. *J. Mol. Catal. A: Chem.* **2007**, *276* (1−2), 162−167.
(31) Jin, G.; Lu, G.; Guo, Y.; Wang, J.; Liu, X. Epoxidation of Propylene by Molecular Oxygen over Modified Ag−MoO_3 Catalyst. *Catal. Lett.* **2003**, *87* (3−4), 249−252.
(32) Lu, J.; Bravo-Suárez, J. J.; Haruta, M.; Oyama, S. T. Direct Propylene Epoxidation over Modified $Ag/CaCO_3$ Catalysts. *Appl. Catal., A* **2006**, *302* (2), 283−295.
(33) Bere, K. E.; Wakui, Y.; Niwa, S.; Shoji, H.; Sato, K.; Hamakawa, S.; Hanaoka, T.; Suzuki, T. M.; Mizukami, F. Direct O_2 Epoxidation of Propylene by the Membrane Reactor Loaded with Ag−Sr Catalyst. *Chem. Lett.* **2007**, *36* (9), 1170−1171.
(34) Triwahyono, S.; Jalil, A. A.; Nur, H.; Hamdan, H.; Kobayashi, M.; Engineering, N. R.; Enginering, E. Development of Membrane Reactor for Epoxidation of Propylene To Propylene Oxide in a Single Step Process. *J. Inst. Eng. Malaysia* **2006**, *67* (3), 1−6.
(35) Golman, B.; Shinoahara, K.; Kobayashi, M. Selectivity and Yield of Exothermic Consecutive Reactions in Catalytically Active Porous Membrane Reactor. *J. Chem. Eng. Jpn.* **1997**, *30* (3), 507−513.
(36) Hazbun, E. A. Ceramic Membrane for Hydrocarbon Conversion. US4791079, 1988.
(37) Gaffney, A.; Jewson, J.; Kahn, A.; Cooker, B. Epoxidation Process Using Supported Silver Catalysts Treated with Carbon Dioxide. WO 99/32471, 1999.
(38) Cooker, B.; Gaffney, A.; Jewson, J.; Kahn, A.; Pitchai, R. Epoxidation Process Using Supported Silver Catalysts Pretreated with Organic Chloride. WO 98/58920, 1998.

(39) Harris, J. W.; Herron, J. A.; DeWilde, J. F.; Bhan, A. Molecular Characteristics Governing Chlorine Deposition and Removal on Promoted Ag Catalysts during Ethylene Epoxidation. *J. Catal.* **2019**, *377*, 378−388.
(40) Zheng, X.; Zhang, Q.; Guo, Y. Y.; Zhan, W.; Guo, Y. Y.; Wang, Y.; Lu, G. Epoxidation of Propylene by Molecular Oxygen over Supported Ag−Cu Bimetallic Catalysts with Low Ag Loading. *J. Mol. Catal. A: Chem.* **2012**, *357*, 106−111.
(41) Ghosh, S.; Acharyya, S. S.; Tiwari, R.; Sarkar, B.; Singha, R. K.; Pendem, C.; Sasaki, T.; Bal, R. Selective Oxidation of Propylene to Propylene Oxide over Silver-Supported Tungsten Oxide Nanostructure with Molecular Oxygen. *ACS Catal.* **2014**, *4* (7), 2169−2174.
(42) Lee, E. J.; Lee, J.; Seo, Y.-J.; Lee, J. W.; Ro, Y.; Yi, J.; Song, I. K. Direct Epoxidation of Propylene to Propylene Oxide with Molecular Oxygen over Ag−Mo−W/ZrO_2 Catalysts. *Catal. Commun.* **2017**, *89*, 156−160.
(43) Yu, B.; Ayvalı, T.; Raine, E.; Li, T.; Li, M. M.-J.; Zheng, J.; Wu, S.; Bagabas, A. A.; Tsang, S. C. E. Enhanced Propylene Oxide Selectivity for Gas Phase Direct Propylene Epoxidation by Lattice Expansion of Silver Atoms on Nickel Nanoparticles. *Appl. Catal., B* **2019**, *243*, 304−312.
(44) Molina, L. M.; Lee, S.; Sell, K.; Barcaro, G.; Fortunelli, A.; Lee, B.; Seifert, S.; Winans, R. E.; Elam, J. W.; Pellin, M. J. Size-Dependent Selectivity and Activity of Silver Nanoclusters in the Partial Oxidation of Propylene to Propylene Oxide and Acrolein: A Joint Experimental and Theoretical Study. *Catal. Today* **2011**, *160* (1), 116−130.
(45) Song, Y.-Y.; Wang, G.-C. Theoretical Study of Propylene Epoxidation over Cu_2O(111) Surface: Activity of O^{2-}, O^-, and O_2^- Species. *J. Phys. Chem. C* **2018**, *122* (37), 21500−21513.
(46) Zhao, B.; Wang, G.-C. C. Theoretical Investigation of Propylene Epoxidation on Ag(111) by Molecular Oxygen: Na(K,Cl) Effects. *J. Phys. Chem. C* **2019**, *123* (28), 17273−17282.
(47) Xiao, T.-T.; Li, R.-S.; Wang, G.-C. A DFT Study and Microkinetic Simulation in Propylene Oxidation on the "29" Cu_xO/Cu(111) Surface. *J. Phys. Chem. C* **2020**, *124* (12), 6611−6623.
(48) Medlin, J. W.; Barteau, M. A. The Formation of Epoxides from Reactions of Oxametallacycles on Ag(110): A Density Functional Theory Study. *J. Phys. Chem. B* **2001**, *105* (41), 10054−10061.
(49) Atmaca, D. O.; Düzenli, D.; Ozbek, M. O.; Onal, I. A Density Functional Theory Study of Propylene Epoxidation on RuO_2 (110) Surface. *Appl. Surf. Sci.* **2016**, *385*, 99−105.
(50) Dai, Y.; Chen, Z.; Guo, Y.; Lu, G.; Zhao, Y.; Wang, H.; Hu, P. Significant Enhancement of the Selectivity of Propylene Epoxidation for Propylene Oxide: A Molecular Oxygen Mechanism. *Phys. Chem. Chem. Phys.* **2017**, *19* (36), 25129−25139.
(51) Kizilkaya, A. C.; Senkan, S.; Onal, I. Investigation of Ruthenium−Copper Bimetallic Catalysts for Direct Epoxidation of Propylene: A DFT Study. *J. Mol. Catal. A: Chem.* **2010**, *330* (1−2), 107−111.
(52) Xu, X.; Friend, C. M. Partial Oxidation without Allylic Carbon-Hydrogen Bond Activation: The Conversion of Propene to Acetone on Rhodium(111)-p(2.Times.1)-O. *J. Am. Chem. Soc.* **1991**, *113* (18), 6779−6785.
(53) Brown, N. F.; Barteau, M. A. Epoxides as Probes of Oxametallacycle Chemistry on Rh(111). *Surf. Sci.* **1993**, *298* (1), 6−17.
(54) Medlin, J. W.; Mavrikakis, M.; Barteau, M. A. Stabilities of Substituted Oxametallacycle Intermediates: Implications for Regioselectivity of Epoxide Ring Opening and Olefin Epoxidation. *J. Phys. Chem. B* **1999**, *103* (50), 11169−11175.
(55) Llorca, J.; Dominguez, M.; Ledesma, C.; Chimentao, R.; Medina, F.; Sueiras, J.; Angurell, I.; Seco, M.; Rossell, O. Propene Epoxidation over TiO_2-Supported Au−Cu Alloy Catalysts Prepared from Thiol-Capped Nanoparticles. *J. Catal.* **2008**, *258* (1), 187−198.
(56) Roldan, A.; Torres, D.; Ricart, J. M.; Illas, F. On the Effectiveness of Partial Oxidation of Propylene by Gold: A Density Functional Theory Study. *J. Mol. Catal. A: Chem.* **2009**, *306* (1−2), 6−10.
(57) Pu, T.; Tian, H.; Ford, M. E.; Rangarajan, S.; Wachs, I. E. Overview of Selective Oxidation of Ethylene to Ethylene Oxide by Ag Catalysts. *ACS Catal.* **2019**, *9* (12), 10727−10750.
(58) Torres, D.; Lopez, N.; Illas, F.; Lambert, R. M. Low-Basicity Oxygen Atoms: A Key in the Search for Propylene Epoxidation Catalysts. *Angew. Chem., Int. Ed.* **2007**, *46* (12), 2055−2058.
(59) Cheng, L.; Yin, C.; Mehmood, F.; Liu, B.; Greeley, J.; Lee, S.; Lee, B.; Seifert, S.; Winans, R. E.; Teschner, D.; Schlögl, R.; Vajda, S.; Curtiss, L. A. Reaction Mechanism for Direct Propylene Epoxidation by Alumina-Supported Silver Aggregates: The Role of the Particle/Support Interface. *ACS Catal.* **2014**, *4* (1), 32−39.
(60) Feng, X.; Yang, J.; Duan, X.; Cao, Y.; Chen, B.; Chen, W.; Lin, D.; Qian, G.; Chen, D.; Yang, C.; Zhou, X. Enhanced Catalytic Performance for Propene Epoxidation with H_2 and O_2 over Bimetallic Au−Ag/Uncalcined Titanium Silicate-1 Catalysts. *ACS Catal.* **2018**, *8* (9), 7799−7808.
(61) Tezsevin, I.; van Santen, R. A.; Onal, I. A Density Functional Theory Study of Propylene Epoxidation Mechanism on Ag_2O(001) Surface. *Phys. Chem. Chem. Phys.* **2018**, *20* (41), 26681−26687.
(62) Fellah, M. F.; Onal, I. Epoxidation of Propylene on a $[Ag_{14}O_9]$ Cluster Representing Ag_2O (001) Surface: A Density Functional Theory Study. *Catal. Lett.* **2012**, *142* (1), 22−31.
(63) Billingsley, D. S.; Holland, C. D. Oxidation of Propylene with Air Over Copper Oxide Catalyst. *Ind. Eng. Chem. Fundam.* **1963**, *2* (4), 252−257.
(64) Wood, B. J.; Wise, H.; Yolles, R. S. Selectivity and Stoichiometry of Copper Oxide in Propylene Oxidation. *J. Catal.* **1969**, *15* (4), 355−362.
(65) Holbrook, L. Mechanism of Promoter Action in Catalytic Oxidation of Propylene to Acrolein*1. *J. Catal.* **1971**, *20* (3), 367−373.
(66) Gentry, S. The Catalytic Properties of Zeolite X Containing Transition Metal Ions III. Propylene Oxidation. *J. Catal.* **1974**, *35* (3), 376−382.
(67) Inui, T. Influence of Retardation Caused by Partially Oxidized Adsorbate upon the Oxidation State of Copper Catalyst and Its Performance for Selective Propylene Oxidation. *J. Catal.* **1980**, *65* (1), 166−173.
(68) Self, D. E.; Oakes, J. D.; White, M. G. Selective Propylene Oxidation over a Copper-Tin Oxide Catalyst. *AIChE J.* **1983**, *29* (4), 625−631.
(69) McCain, C. C.; Godin, G. W. Detection of Homogeneous Reactions in the Presence of Heterogeneous Catalytic Reaction. *Nature* **1964**, *202* (4933), 692−693.
(70) Daniel, C. The Catalytic Oxidation of Propylene I. Evidence for Surface Initiated Homogeneous Reactions. *J. Catal.* **1972**, *24* (3), 529−535.
(71) Shindo, T.; Inoue, H. Formation of Propylene Oxide in the Catalytic Oxidation of Propylene. *Nippon Kagaku Kaishi* **1978**, *3*, 468−469.
(72) Orzesek, H.; Schulz, R. P.; Dingerdissen, U.; Maier, W. F. Selective Oxidation of Propene with Air to Propylene Oxide, a Case Study of Autoxidation Versus Catalytic Oxidation with AMM-Catalysts. *Chem. Eng. Technol.* **1999**, *22* (8), 691−700.
(73) Teržan, J.; Djinović, P.; Zavašnik, J.; Arčon, I.; Žerjav, G.; Spreitzer, M.; Pintar, A. Alkali and Earth Alkali Modified CuO_x/SiO_2 Catalysts for Propylene Partial Oxidation: What Determines the Selectivity? *Appl. Catal., B* **2018**, *237*, 214−227.
(74) Marimuthu, A.; Zhang, J.; Linic, S. Tuning Selectivity in Propylene Epoxidation by Plasmon Mediated Photo-Switching of Cu Oxidation State. *Science (Washington, DC, U. S.)* **2013**, *339* (6127), 1590−1593.
(75) Kalyoncu, Ş.; Düzenli, D.; Onal, I.; Seubsai, A.; Noon, D.; Senkan, S.; Say, Z.; Vovk, E. I.; Ozensoy, E. NaCl-Promoted CuO−RuO_2/SiO_2 Catalysts for Propylene Epoxidation with O_2 at Atmospheric Pressures: A Combinatorial Micro-Reactor Study. *Catal. Lett.* **2015**, *145* (2), 596−605.
(76) Yang, L.; He, J.; Zhang, Q.; Wang, Y. Copper-Catalyzed Propylene Epoxidation by Oxygen: Significant Promoting Effect of

https://dx.doi.org/10.1021/acscatal.0c03340
ACS Catal. 2020, 10, 13415−13436

Vanadium on Unsupported Copper Catalyst. *J. Catal.* **2010**, *276* (1), 76−84.
(77) Schulz, K. H.; Cox, D. F. Propene Adsorption on Cu_2O Single-Crystal Surfaces. *Surf. Sci.* **1992**, *262* (3), 318−334.
(78) Schulz, K. H.; Cox, D. F. Propene Oxidation over Cu_2O Single-Crystal Surfaces: A Surface Science Study of Propene Activation at 1 Atm and 300 K. *J. Catal.* **1993**, *143*, 464−480.
(79) Reitz, J. B.; Solomon, E. I. Propylene Oxidation on Copper Oxide Surfaces: Electronic and Geometric Contributions to Reactivity and Selectivity. *J. Am. Chem. Soc.* **1998**, *120* (44), 11467−11478.
(80) Su, W.; Shi, Y.; Zhang, C.; Wang, W.; Song, X.; Bai, Y.; Wang, J.; Yu, G. Size Effect of Unsupported CuO_x on Propylene Epoxidation by Oxygen. *Catal. Lett.* **2020**, *150* (4), 939−947.
(81) Wang, Y.; Chu, H.; Zhu, W.; Zhang, Q. Copper-Based Efficient Catalysts for Propylene Epoxidation by Molecular Oxygen. *Catal. Today* **2008**, *131* (1−4), 496−504.
(82) Wang, Q.; Zhan, C.; Zhou, L.; Fu, G.; Xie, Z. Effects of Cl^- on Cu_2O Nanocubes for Direct Epoxidation of Propylene by Molecular Oxygen. *Catal. Commun.* **2020**, *135*, 105897.
(83) Vaughan, O.; Kyriakou, G.; MacLeod, N.; Tikhov, M.; Lambert, R. Copper as a Selective Catalyst for the Epoxidation of Propene. *J. Catal.* **2005**, *236* (2), 401−404.
(84) He, J.; Zhai, Q.; Zhang, Q.; Deng, W.; Wang, Y. Active Site and Reaction Mechanism for the Epoxidation of Propylene by Oxygen over CuO_x/SiO_2 Catalysts with and without Cs^+ Modification. *J. Catal.* **2013**, *299*, 53−66.
(85) Yang, X.; Kattel, S.; Xiong, K.; Mudiyanselage, K.; Rykov, S.; Senanayake, S. D.; Rodriguez, J. A.; Liu, P.; Stacchiola, D. J.; Chen, J. G. Direct Epoxidation of Propylene over Stabilized Cu^+ Surface Sites on Titanium-Modified Cu_2O. *Angew. Chem., Int. Ed.* **2015**, *54* (41), 11946−11951.
(86) Diekmann, M.; Koch, G.; König, M.; Ressler, T. Correlation between Copper Oxide Particle Size and Selectivity towards Propylene Oxide in Selective Oxidation of Propene. *ChemCatChem* **2018**, *10* (23), 5459−5467.
(87) Seubsai, A.; Noon, D.; Chukeaw, T.; Zohour, B.; Donphai, W.; Chareonpanich, M.; Senkan, S. Epoxidation of Propylene to Propylene Oxide with Molecular Oxygen over Sb_2O_3−CuO−NaCl/SiO_2 Catalysts. *J. Ind. Eng. Chem.* **2015**, *32*, 292−297.
(88) Seubsai, A.; Uppala, C.; Tiencharoenwong, P.; Chukeaw, T.; Chareonpanich, M.; Zohour, B.; Noon, D.; Senkan, S. High Stability of Ruthenium−Copper-Based Catalysts for Epoxidation of Propylene. *Catal. Lett.* **2018**, *148* (2), 586−600.
(89) Harris, J. W.; Bhan, A. Kinetics of Chlorine Deposition and Removal over Promoted Silver Catalysts during Ethylene Epoxidation. *J. Catal.* **2019**, *380*, 318−331.
(90) Teržan, J.; Huš, M.; Arčon, I.; Likozar, B.; Djinović, P. Effect of Na, Cs and Ca on Propylene Epoxidation Selectivity over CuO_x/SiO_2 Catalysts Studied by Catalytic Tests, in-Situ XAS and DFT. *Appl. Surf. Sci.* **2020**, *528*, 146854.
(91) Song, Y.-Y.; Wang, G.-C. A DFT Study and Microkinetic Simulation of Propylene Partial Oxidation on CuO (111) and CuO (100) Surfaces. *J. Phys. Chem. C* **2016**, *120* (48), 27430−27442.
(92) Song, Y.-Y.; Dong, B.; Wang, S.-W.; Wang, Z.-R.; Zhang, M.; Tian, P.; Wang, G.-C.; Zhao, Z. Selective Oxidation of Propylene on Cu_2O(111) and Cu_2O(110) Surfaces: A Systematically DFT Study. *ACS Omega* **2020**, *5* (12), 6260−6269.
(93) Hammer, B.; Norskov, J. K. Why Gold Is the Noblest of All the Metals. *Nature* **1995**, *376* (6537), 238−240.
(94) Kopač, D.; Likozar, B.; Huš, M. How Size Matters: Electronic, Cooperative, and Geometric Effect in Perovskite-Supported Copper Catalysts for CO_2 Reduction. *ACS Catal.* **2020**, *10* (7), 4092−4102.
(95) Bickelhaupt, F. M.; Houk, K. N. Analyzing Reaction Rates with the Distortion/Interaction-Activation Strain Model. *Angew. Chem., Int. Ed.* **2017**, *56* (34), 10070−10086.
(96) Moens, B.; Dewinne, H.; Corthals, S.; Poelman, H.; Degryse, R.; Meynen, V.; Cool, P.; Sels, B.; Jacobs, P. Epoxidation of Propylene with Nitrous Oxide on Rb_2SO_4-Modified Iron Oxide on Silica Catalysts. *J. Catal.* **2007**, *247* (1), 86−100.
(97) Ananieva, E.; Reitzmann, A. Direct Gas-Phase Epoxidation of Propene with Nitrous Oxide over Modified Silica Supported FeO_x Catalysts. *Chem. Eng. Sci.* **2004**, *59* (22−23), 5509−5517.
(98) Jeong, N. C.; Lee, J. S.; Tae, E. L.; Lee, Y. J.; Yoon, K. B. Acidity Scale for Metal Oxides and Sanderson's Electronegativities of Lanthanide Elements. *Angew. Chem., Int. Ed.* **2008**, *47* (52), 10128−10132.
(99) Liu, J.-C.; Tang, Y.; Chang, C.-R.; Wang, Y.-G.; Li, J. Mechanistic Insights into Propene Epoxidation with O_2−H_2O Mixture on Au_7/α-Al_2O_3: A Hydroproxyl Pathway from Ab Initio Molecular Dynamics Simulations. *ACS Catal.* **2016**, *6* (4), 2525−2535.
(100) Kwon, S.; Deshlahra, P.; Iglesia, E. Reactivity and Selectivity Descriptors of Dioxygen Activation Routes on Metal Oxides. *J. Catal.* **2019**, *377*, 692−710.
(101) van Deelen, T. W.; Hernández Mejía, C.; de Jong, K. P. Control of Metal-Support Interactions in Heterogeneous Catalysts to Enhance Activity and Selectivity. *Nat. Catal.* **2019**, *2* (11), 955−970.
(102) Carbonio, E. A.; Rocha, T. C. R.; Klyushin, A. Y.; Píš, I.; Magnano, E.; Nappini, S.; Piccinin, S.; Knop-Gericke, A.; Schlögl, R.; Jones, T. E. Are Multiple Oxygen Species Selective in Ethylene Epoxidation on Silver? *Chem. Sci.* **2018**, *9* (4), 990−998.
(103) Jones, T. E.; Rocha, T. C. R.; Knop-Gericke, A.; Stampfl, C.; Schlögl, R.; Piccinin, S. Thermodynamic and Spectroscopic Properties of Oxygen on Silver under an Oxygen Atmosphere. *Phys. Chem. Chem. Phys.* **2015**, *17* (14), 9288−9312.
(104) Li, W.-X.; Stampfl, C.; Scheffler, M. Why Is a Noble Metal Catalytically Active? The Role of the O-Ag Interaction in the Function of Silver as an Oxidation Catalyst. *Phys. Rev. Lett.* **2003**, *90* (25), 256102.
(105) Li, W.-X.; Stampfl, C.; Scheffler, M. Insights into the Function of Silver as an Oxidation Catalyst by Ab Initio Atomistic Thermodynamics. *Phys. Rev. B: Condens. Matter Mater. Phys.* **2003**, *68* (16), 165412.
(106) Stegelmann, C.; Schiødt, N. C.; Campbell, C. T.; Stoltze, P. Microkinetic Modeling of Ethylene Oxidation over Silver. *J. Catal.* **2004**, *221* (2), 630−649.
(107) Kahn, A.; Gaffney, A.; Pitchai, R. Propylene Oxide Process Using Alkaline Earth Metal Compound-Supported Silver Catalysts. WO 97/34693, 1997.
(108) Cited, R.; Documents, U. S. P. Propylene Oxide Process Using Alkaline Earth Metal Compound-Supported Silver Catalysts Containing Tungsten and Potassium Promoters. WO 98/52931, 1999.
(109) Bal, R.; Ghosh, S.; Shanka, G. A.; Sarkar, B.; Pendem, C.; Singha, R. K. Process for Preparation of Ag-W Oxide Catalyst for the Selective Conversion of Propropylene to Propylene Oxide with Molecular Oxygen. WO 2013/098855 A1, 2012.
(110) Wang, S.; Omidvar, N.; Marx, E.; Xin, H. Coordination Numbers for Unraveling Intrinsic Size Effects in Gold-Catalyzed CO Oxidation. *Phys. Chem. Chem. Phys.* **2018**, *20* (9), 6055−6059.
(111) Klemm, E.; Dietzsch, E.; Schwarz, T.; Kruppa, T.; De Oliveira, A. L.; Becker, F.; Markowz, G.; Schirrmeister, S.; Schütte, R.; Caspary, K. J.; Schüth, F.; Hönicke, D. Direct Gas-Phase Epoxidation of Propene with Hydrogen Peroxide on TS-1 Zeolite in a Microstructured Reactor. *Ind. Eng. Chem. Res.* **2008**, *47* (6), 2086−2090.
(112) Perez Ferrandez, D. M.; de Croon, M. H. J. M.; Schouten, J. C.; Nijhuis, T. A. Gas-Phase Epoxidation of Propene with Hydrogen Peroxide Vapor. *Ind. Eng. Chem. Res.* **2013**, *52* (30), 10126−10132.

https://dx.doi.org/10.1021/acscatal.0c03340
ACS Catal. 2020, 10, 13415−13436